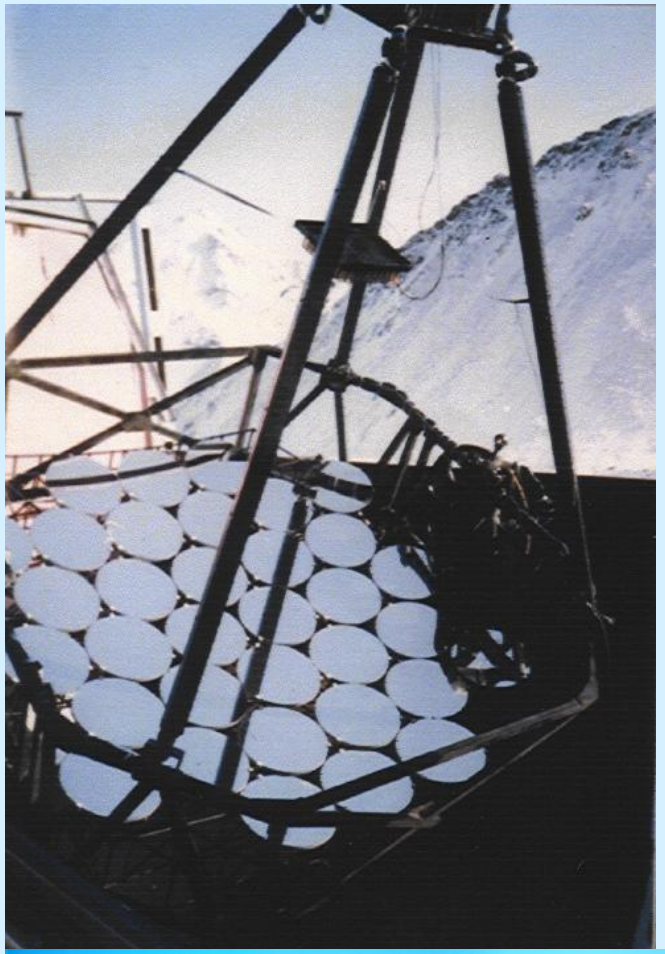

SHALON

V.G. SINITSYNA, V.Y. SINITSYNA

P. N. Lebedev Physical Institute,
Leninsky prospect 53, Moscow, 119991 Russia

VERY-HIGH ENERGY GAMMA-RAY ASTRONOMY of GALACTIC and EXTRA-GALACTIC SOURCES by SHALON

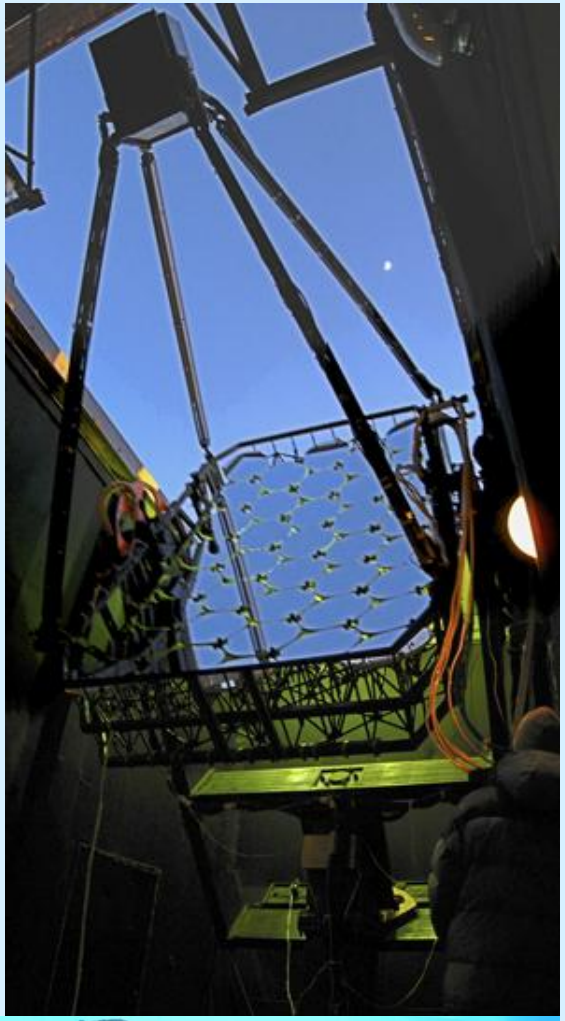

The SHALON Cherenkov gamma-telescope located at 3340 m a.s.l., at the Tien Shan high-mountain observatory of Lebedev Physical Institute, has been developed for gamma - astronomical observation in the energy range 0,8-100 TeV. The gamma – astronomical researches are carrying out with SHALON since 1992. During the period 1992 - 2014 SHALON has been used for observations of metagalactic sources: Mkn 421, Mkn 501, Mkn 180, NGC 1275, SN2006gy, 3c382, OJ 287, 3c454.3, 1739+522 and galactic sources: Crab Nebula, Cyg X-3, Tycho's SNR, Cas A, Geminga, 2129+47XR.


SHALON 2
SHALON 1

HIGH MOUNTAINOUS OBSERVATORY SHALON ALATOO

SHALON mirror Cherenkov telescope created at Lebedev Physical Institute and stated in 1991 - 1992

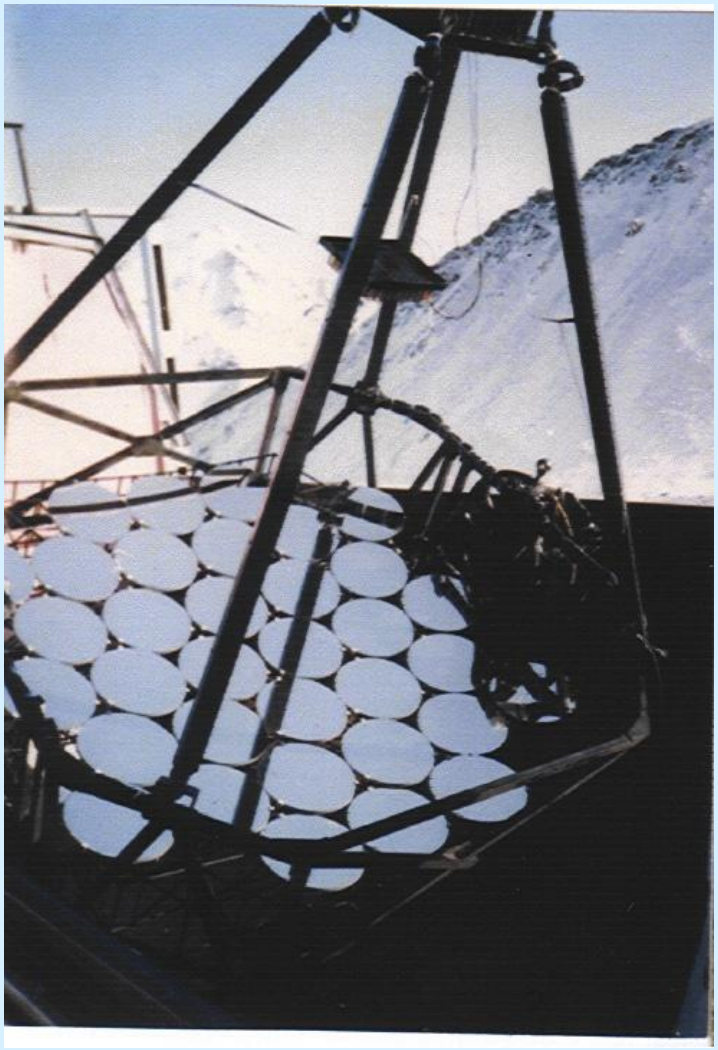

- Total area of spherical mirror — 11.2 m^2
- Radius of mirror curvature — 8.5 m
- The angle range of telescope turn:
  - azimuth — 0^o-360^o
  - zenith — 0^o-110^o
- The accurace of telescopic axis pointing — $\leq 0.1^o$
- The photomultiplier tube camera (12x12) — 144 elements
- Field of view $> 8^o$
- Weigth 6 ton
- altazimuth mounting

It is essential that our telescope has a large matrix with full angle $>8^o$ that allows us to perform observations of the supposed astronomical source (ON data) and background from extensive air showers (EAS) induced by cosmic ray (OFF data) simultaneously. Thus, the OFF data are collecting for exactly the same atmospheric thickness, transparency and other experimental conditions as the ON data.

The lightreceiver has the largest field of view in the world, >8°. This allows one to monitor the background from charged cosmic-ray particles and the atmospheric transparency continuously during observations and expands the area of observation and, hence, the efficiency of observations. The technique for simultaneously obtaining information about the cosmic-ray background and the showers initiated by gamma rays is unique and has been applied in the SHALON experiment from the very beginning of its operation. This technique serves to increase the useful source tracking time and, what is particularly important, such source and background observation conditions as the thickness and state of the atmosphere remain the same.

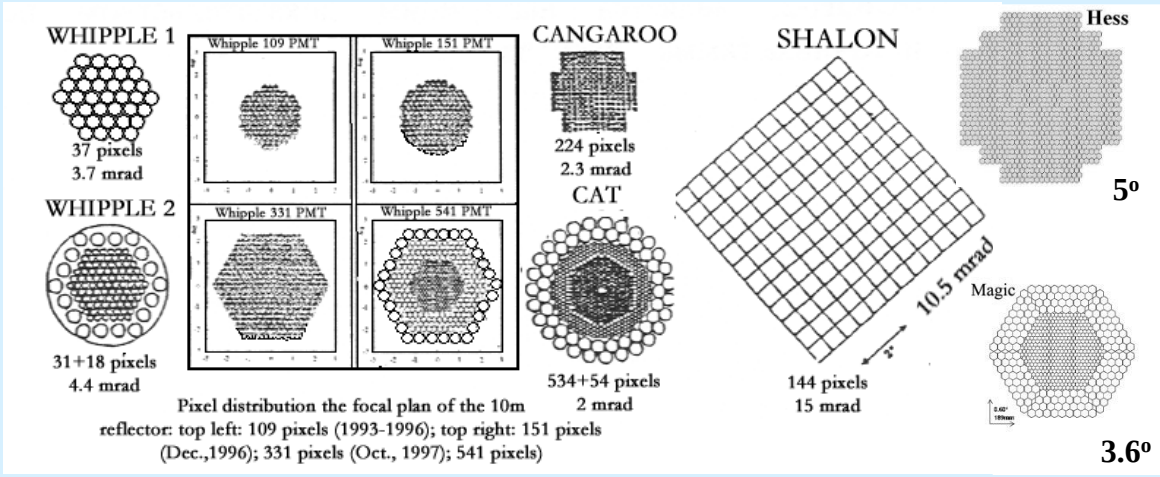

Pixel distribution the focal plan of the 10m reflector: top left: 109 pixels (1993-1996); top right: 151 pixels (Dec.,1996); 331 pixels (Oct., 1997); 541 pixels)

This method is inaccessible to other gamma-ray astronomical experiments, because the telescopes used in the world have a smaller field of view. In addition, the wide field of view allows recording the off-center showers arriving at distances of more than 30 m from the telescope axis completely and almost without any distortions; they account for more 90% of all the showers recorded by the telescope.

During a primary analysis, the primary particle arrival direction is determined with an accuracy up to ≤0.1°. The subsequent analysis specially developed for the SHALON telescopes and based on Tikhonov's regularization method improves the accuracy to a value of less than 0.01°.

SHALON sky-map catalogue of γ -quantum sources 800 GeV – 100TeV (2013)

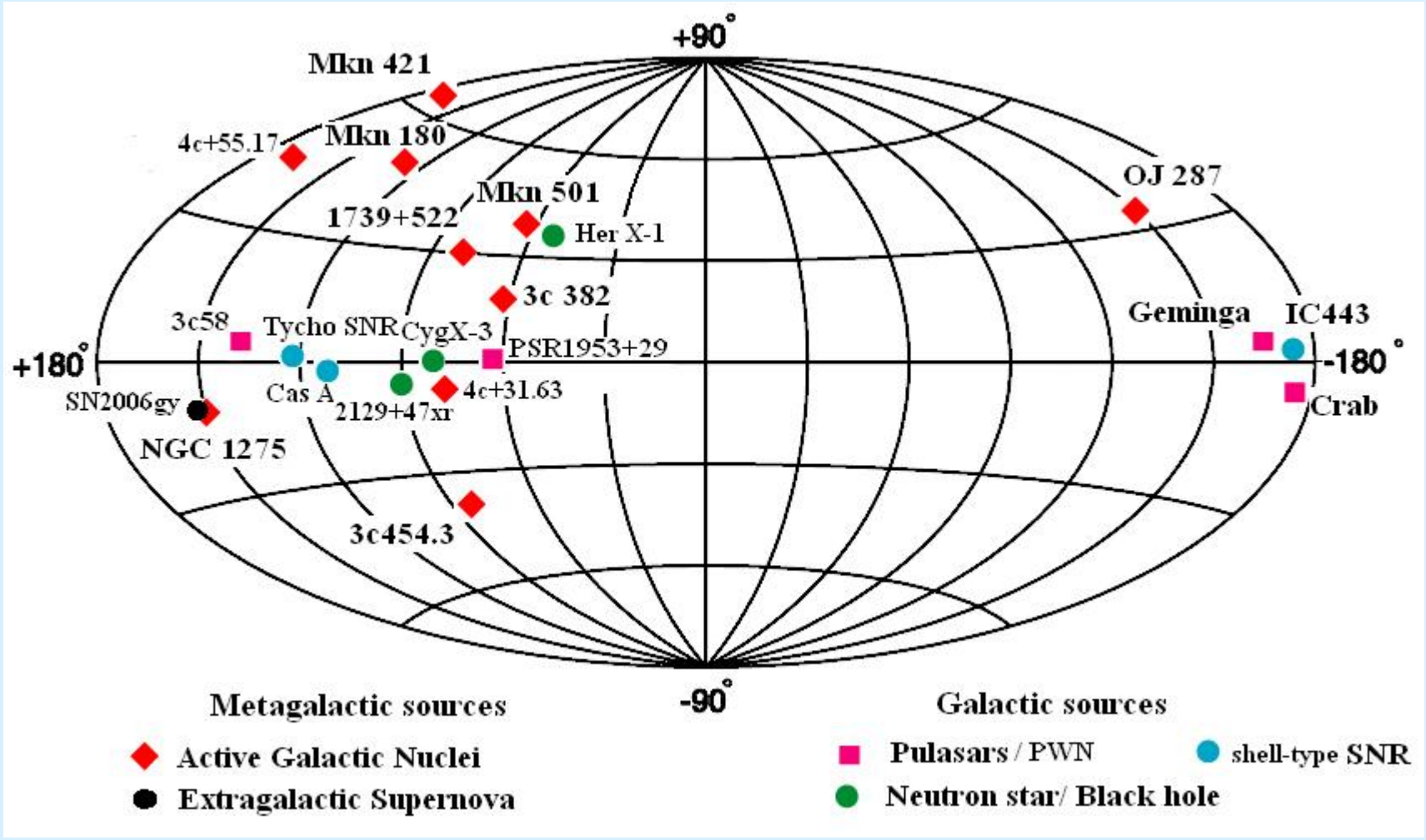

SHALON catalogue of γ -quantum sources 800 GeV – 100TeV (2014)

Source	Source type	Observed Flux, $cm^{-2}s^{-1}$	Distance		Detected** by SHALON	Detected at high energies Experiment/year	Detected at very high energies Experiment/year
Galactic			***kpc***				
Crab Nebula	Plerion, PWN	$(2.12\pm0.12)\times10^{-12}$	2.0		1995[1]	COS-B/1987 [15] (FermiLAT/2009)	Whipple/1989 [16]
* Geminga	Radio-weak pulsar/ Plerion (?)	$(0.48\pm0.07)\times10^{-12}$	0.25		2000[5]	COS-B/1981 [18] EGRET/1994 [19] (FermiLAT/2009)	Crimea/2001 [49] MILAGRO/2007 [20]
*GK Per (Nova 1901)	Classical nova/SNR	$(0.31\pm0.14)\times10^{-12}$	0.46		2014		
* 3c 58	Plerion, PWN	$(0.56\pm0.15)\times10^{-12}$	2.6 - 3.2		2012[14]	FermiLAT/2009 [27]	*(VERITAS/2006 UL)*
SNR 1181 (?)	Plerion, PWN (?)	$(1.40\pm0.43)\times10^{-12}$	2.6 - 3.2 (?)		2012[14]	FermiLAT/2009 [27]	–
* Tycho's SNR	Shell-type SNR	$(0.52\pm0.04)\times10^{-12}$	2.5 – 3,5		1998[4]	FermiLAT/2011 [24]	VERITAS/2011 [23]
Cas A	Shell-type SNR	$(0.64\pm0.10)\times10^{-12}$	3,1		2011[12]	FermiLAT/2010 [26]	HEGRA/2001 [25]
IC 443	Shell-type SNR	$(1.69\pm0.58)\times10^{-12}$	1.5		2012[14]	EGRET/1996 [21] (FermiLAT/2009)	MAGIC/2007 [22]
* γCygni SNR	Shell-type SNR	$(1.27\pm0.11)\times10^{-12}$	1.5		2013 [50]	EGRET/1996 [21] (FermiLAT/2009)	VERITAS/2013 [51]
* Cygnus X-3	Binary	$(0.68\pm0.04)\times10^{-12}$	10		1997[2]	EGRET/1997[29] (FermiLAT/2009[30])	Crimea/2009 [48] (*Crimea/1975* [28])
* 2129+47XR	Low-mass X-ray Binary	$(0.19\pm0.06)\times10^{-12}$	6.0		2006[7]	–	–
* Her X-1	Binary	$(0.45\pm0.18)\times10^{-12}$	6.6		2012	–	*(Whipple UL)*
* M57	Planetary nebula	$(0.30\pm0.17)\times10^{-12}$	0.7		2011[13]	–	–
Extragalactic			***Mpc***	***z***			
* NGC 1275	Seyfert Galaxy	$(0.78\pm0.05)\times10^{-12}$	71	0.0179	1997[3]	FermiLAT/2009 [31]	MAGIC/2012 [32]
* SN2006 gy	Extragalactic Supernova	$(3.71\pm0.65)\times10^{-12}$	73	0.019	2007[9]	–	–
Mkn 421	BLLac	$(0.63\pm0.05)\times10^{-12}$	124	0.031	1995[1]	EGRET/1992 [35](FermiLAT/2009)	Whipple/1992 [33]
Mkn 501	BLLac	$(0.86\pm0.06)\times10^{-12}$	135	0.034	1997[1a]	EGRET/1999 [37](FermiLAT/2009)	Whipple/1996 [34]
Mkn 180	BLLac	$(0.65\pm0.09)\times10^{-12}$	173	0.046	2009[10]	FermiLAT/2009 [39]	MAGIC/2006 [38]
* 3c382	Broad Line Radio Galaxy	$(0.95\pm0.33)\times10^{-12}$	230	0.058	2010[11]	*(FermiLAT UL)* [40]	–
* 4c+31.63	FSRQ	$(0.72\pm0.22)\times10^{-12}$	1509	0.295	2013	FermiLAT/2010 [47]	–
* OJ 287	BLLac	$(0.26\pm0.07)\times10^{-12}$	1576	0.306	*2005* [8] *(UL)* 2010[11]	FermiLAT/2009 [41]	*(MAGIC / 2009 UL)* [42]
* 3c454.3	FSRQ	$(0.43\pm0.07)\times10^{-12}$	5489	0.859	2000[6]	FermiLAT/2009 [44]	*(MAGIC / 2009 UL)* [45]
* 4c+55.17	FSRQ	$(0.91\pm0.25)\times10^{-12}$	5785	0.896	2013	FermiLAT/2011 [43]	–
* 1739+522 (4c+51.37)	FSRQ	$(0.49\pm0.05)\times10^{-12}$	9913	1.375	2000[6]	FermiLAT/2010 [46]	–

TeV GAMMA-RAY EMISSION from GALACTIC SOURCES

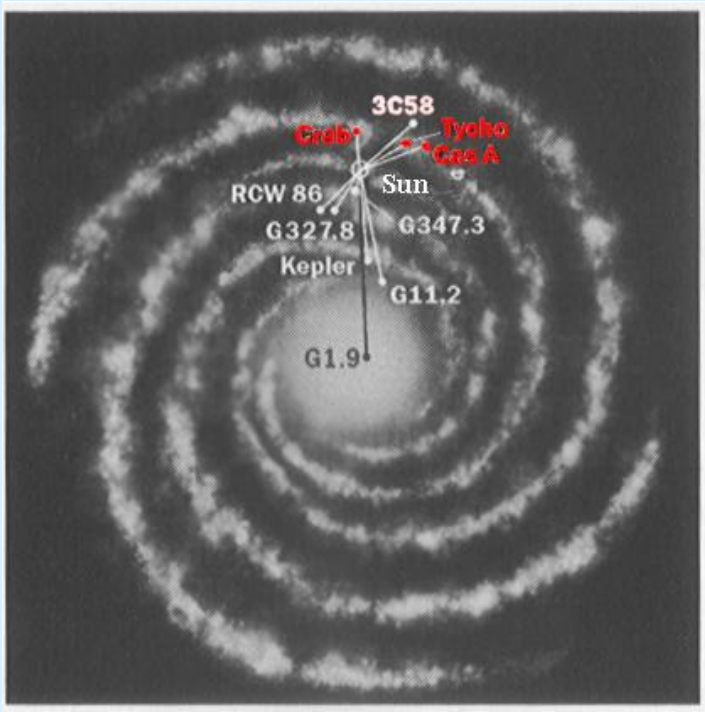

Position of the supposed supernova remnants exploded in the last 2000 years in the Galaxy disk

The hypothesis that Supernova Remnants (SNRs) are unique candidates for cosmic-ray sources has been prevalent from the very outset of cosmic-ray physics. Recent observations of several SNRs in X-rays and TeV *gamma*-rays will help in solving the problem of the origin of cosmic rays and are key to understanding the mechanism of particle acceleration at a propagating shock wave. A number of nearby Northern Hemisphere SNRs (see table) of different types has been observed in TeV energies with SHALON Cherenkov telescope; some of them have been studied in details and the results of observations are presented here.

SNRs observed by SHALON at energies > 800 GeV

Sources	Type	Observable flux, ($cm^{-2}s^{-1}$)	Distance, (kpc)
Crab Nebula	Plerion	$(2.12 \pm 0.11) \times 10^{-12}$	2
*** Geminga**	Radioweak pulsar/PWN	$(0.48 \pm 0.07) \times 10^{-12}$	0.25
***3c58(SN1181)**	Plerion	$(0.54 \pm 0.15) \times 10^{-12}$	2.6 - 3.2
***Tycho's SNR**	Shell type SNR	$(0.52 \pm 0.04) \times 10^{-12}$	2.5 - 3.5
Cas A	Shell type SNR	$(0.74 \pm 0.09) \times 10^{-12}$	3.1
IC 443	Shell type SNR	$(1.69 \pm 0.58) \times 10^{-12}$	1.5
γCygni SNR	Shell type SNR	$(1.27 \pm 0.11) \times 10^{-12}$	1.5

Tycho's SNR (1572yr)

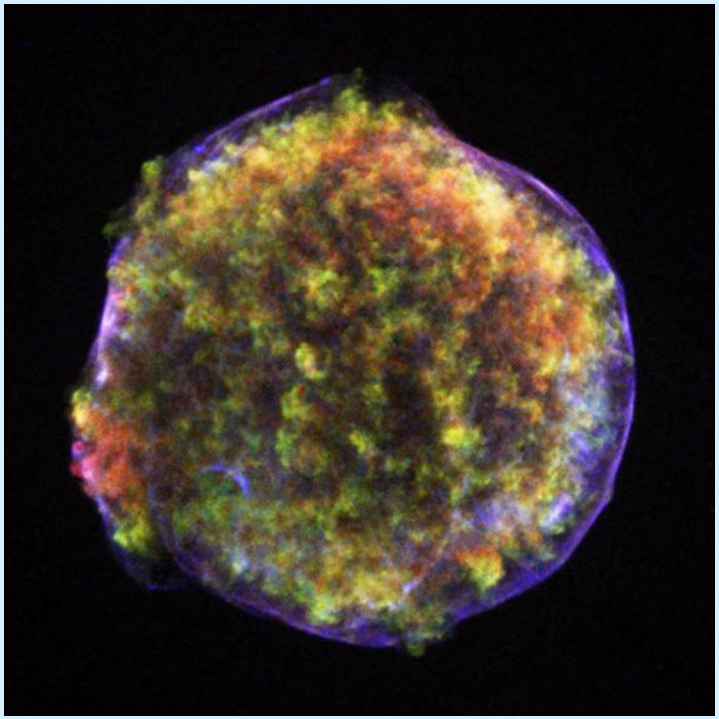

Tycho's SNR has long been considered as a candidate to cosmic ray hadrons source in Northern Hemisphere. Tycho's SNR have been detected with SHALON mirror Cherenkov telescope at TeV region. The integral gamma-ray flux above 0.8 TeV was estimated as: $\mathbf{(0.52\pm0.04)\times10^{-12}\ cm^{-2}s^{-1}}$. with a statistical significance of **17σ** Li&Ma. The *gamma*-ray integral spectrum by SHALON in the energy range of 0.8 – 80 TeV is fitted by a power law with exponential cut-off :

$$\mathbf{I(>E_\gamma)=(0.48\pm0.04)\times10^{-12}\times E_\gamma^{-0.93\pm0.09}\exp(-E_\gamma/35TeV)}$$

Recently, Tycho's SNR was also confirmed with VERITAS telescope in observations of 2008 - 2010 and 2011 years.

Kinetic nonlinear theory of diffusive CR acceleration in SNRs connects the gas dynamics of the explosion with the particle acceleration. The nonlinear kinetic model for cosmic ray acceleration in SNR has been applied to Tycho's SNR in order to describe the Tycho's SNR characteristics.

The expected π^O-decay gamma-quantum flux $F_\gamma \propto E_\gamma^{-1}$ extends up to ~80 TeV, whereas the Inverse Compton gamma-ray flux has a cutoff above the few TeV. So, the detection of gamma-rays at energies of ~ 10-80 TeV by SHALON telescope is the evidence of hadronic origin.

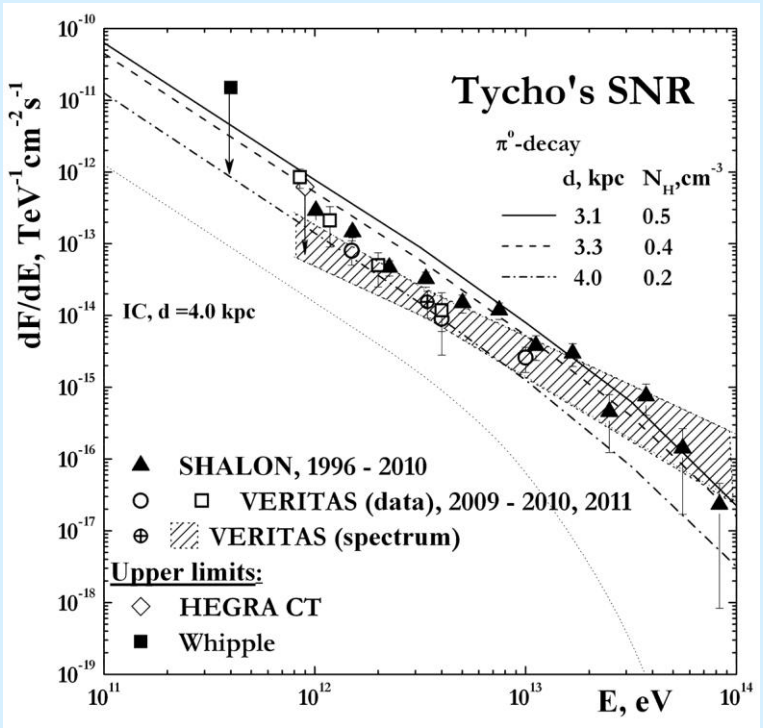

Tycho's SNR

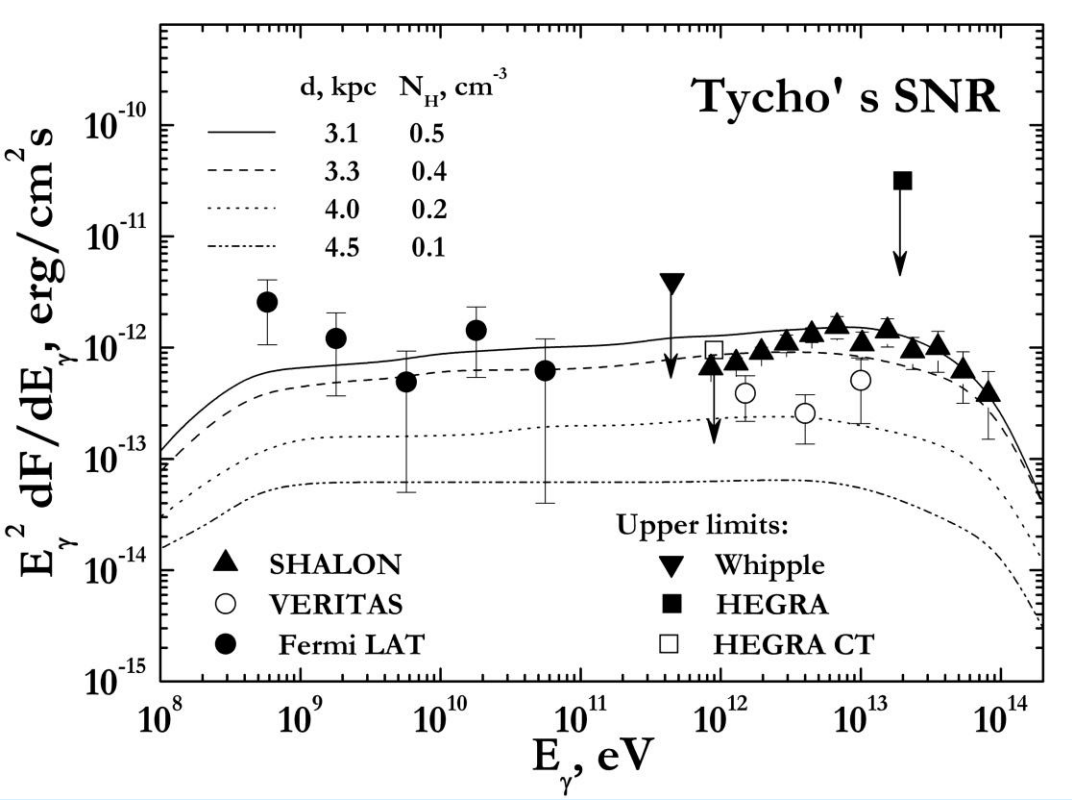

Spectral energy distribution of the γ-ray emission from Tycho's SNR, as a function of γ-ray energy ε_γ, for a mechanical SN explosion energy of $E_{SN} = 1.2\times10^{51}$ erg and four different distances d and corresponding values of the ISM number densities N_H.

The additional information about parameters of Tycho's SNR can be predicted (in frame of this theory) if the TeV gamma-quantum spectrum of SHALON telescope is taken into account: a source distance 3.1 - 3.3 kpc and an ambient density N_H=0.5 - 0.4 cm^{-3} and the expected π^o-decay gamma-ray energy extends up to about 100 TeV

Recently, Tycho's SNR was also detected at GeV energy range by Fermi LAT (●) (2010, 2011). The Tycho's SNR spectral energy distribution by SHALON (▲) (1996 - 2010) comparing with VERITAS (○) (2009), Fermi LAT (●) (2010, 2011) and theoretical models [Volk H.J. Berezhko E.G. Ksenofontov L.T., 2008].

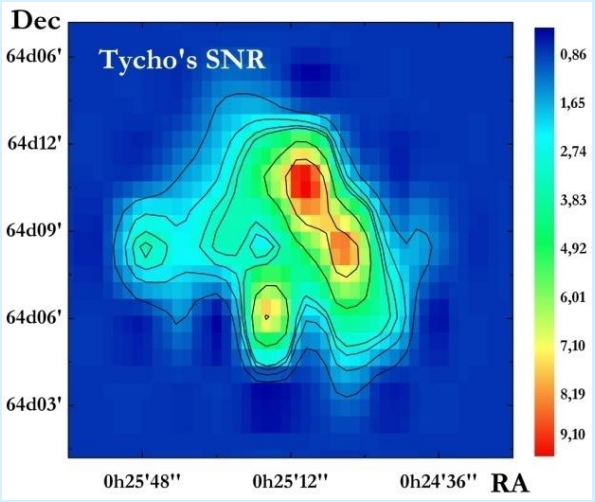

The image of Tycho's SNR by SHALON

Cassiopeia A (1680 yr.)

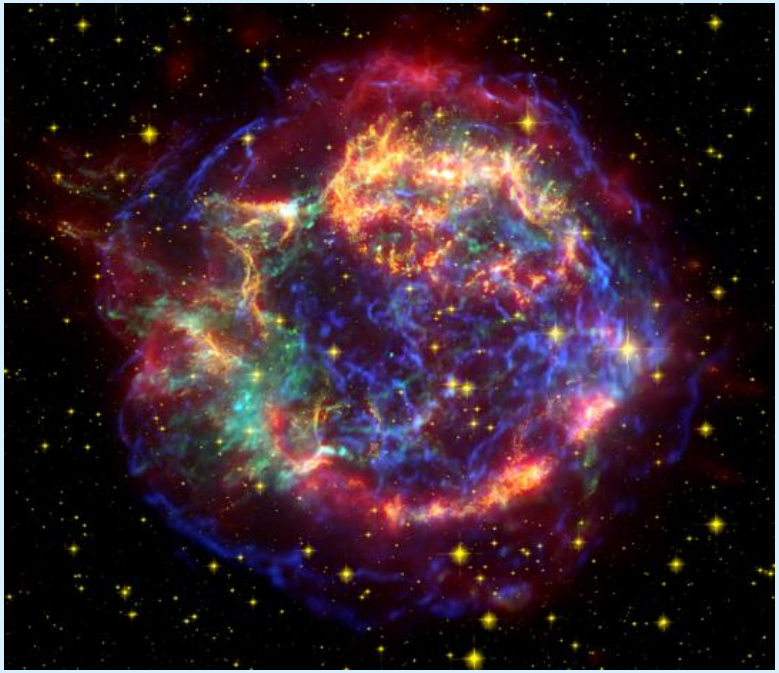

Cassiopeia A (Cas A) is the youngest of historical supernova remnant in our Galaxy. Its overall brightness across the electromagnetic spectrum makes it a unique object for studying high-energy phenomena in SNRs. Cas A was detected in TeV *gamma*-rays, first by HEGRA (2001) and later confirmed by MAGIC (2007) and VERITAS (2010). The high energy *gamma*-ray emission from Cas A was detected with Fermi LAT (2010) in the range 500 MeV - 50 GeV.

The composite image of Cas A SNR.
Infrared data from the Spitzer Space Telescope are colored red;
Optical data from the Hubble Space Telescope are yellow;
X-ray data from the Chandra Observatory are green and blue.

Cas A was observed with SHALON telescope during the 68 hours from 2010 to 2013. All observations were made with the standard procedure of SHALON experiment during moonless nights with zenith angles from 13 to 35 degree. The *gamma*-ray source associated with the SNR Cassiopeia A was detected above 800 GeV with a statistical significance of 13.2σ *Li&Ma* with a *gamma*-quantum flux above 0.8 TeV :

$$\mathbf{I_{CasA}(>0{,}8TeV) = (0{,}64\pm0{,}10)\bullet10^{-12}\ cm^{-2}s^{-1}}$$

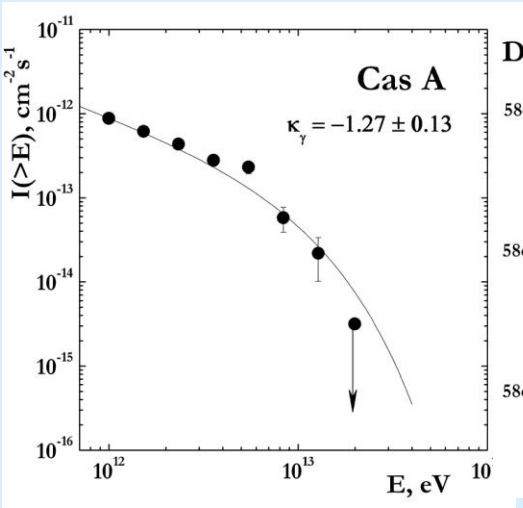

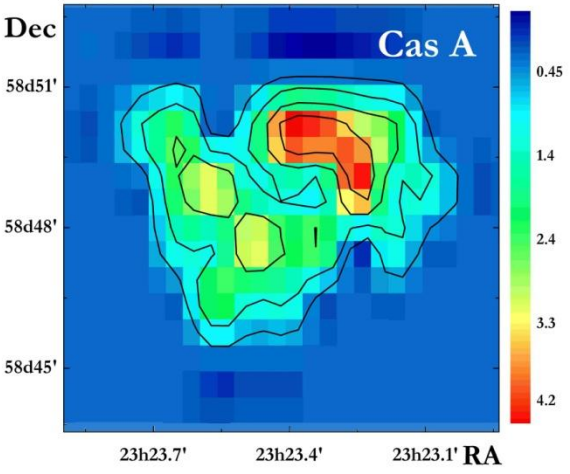

Cassiopeia A

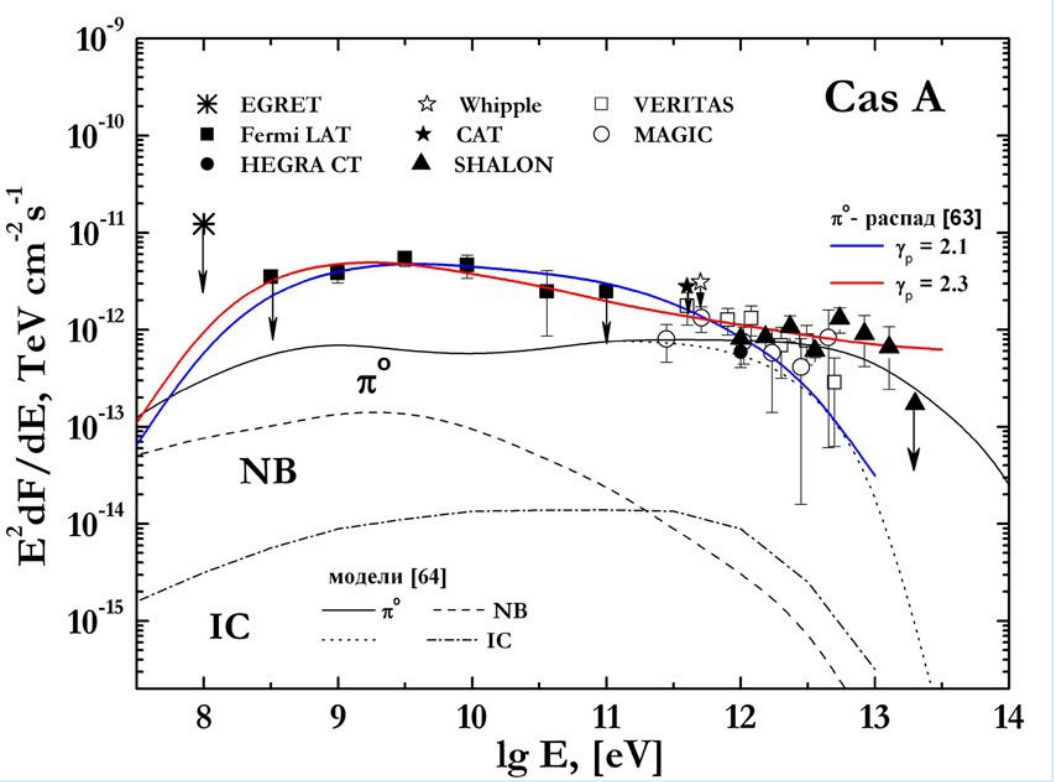

The spectral energy distribution of the γ-ray emission from Cas A by SHALON (▲) in comparison with other experiment data Fermi LAT, HEGRA, MAGIC, VERITAS, EGRET, CAT, Whipple and with theoretical predictions [Abdo A A et al. 2010; Berezhko E G, Pühlhofer G, Völk H J, 2003] .

The favored scenarios in which the *gamma*-rays of 500 MeV – 10 TeV energies are emitted in the shell of the SNR like Cas A are Inverse Compton scattering and π^o-decay. The *gamma*-ray emission could be produced by electrons accelerated at the forward shock through relativistic bremsstrahlung (NB) or IC. Alternatively, the GeV *gamma*-ray emission could be produced by accelerated CR hadrons through interaction with the background gas and then π^o-decay.

Solid lines show the very high energy *gamma*-ray spectra of hadronic origin. Dash-and-dot line presents the *gamma*-ray spectrum of the IC emission. It was shown that leptonic model with B = 0.3 mG predicts a 5 - 8 times lower *gamma*-ray flux than the observed; the model with B = 0.12 mG, which can broadly explain the observed GeV flux predicts the TeV spectrum with cut-off energy about 10 TeV.

The detection of very high energy *gamma*-ray emission at 5 - 15 TeV and the hard spectrum below 1 TeV would favor the πo-decay origin of the *gamma*-rays in Cas A SNR

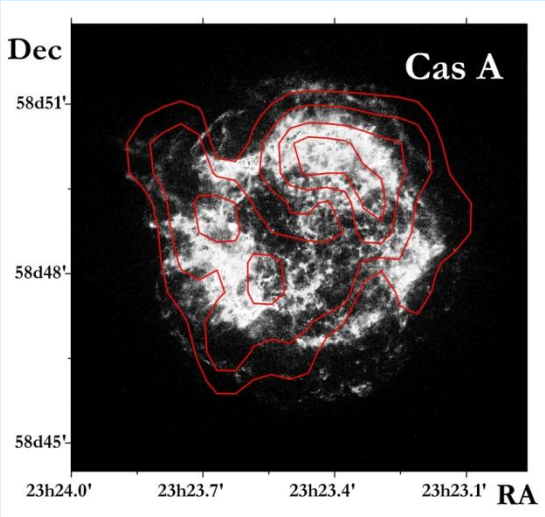

Chandra image of Cas A (X-ray);
The contour lines show the TeV-image by SHALON

IC 443 age of (3 ÷ 30)×10^3yr.

The composite image of IC 443 SNR.

Radio data from the Dominion Radio Astrophysical Observatory are colored green;
Optical data from the Digitized Sky Survey are red;
X-ray data from the Chandra X-ray Observatory are blue.

The supernova remnant (SNR) IC 443 is well known for its radio, optical, X-ray, and MeV-TeV energy gamma-ray emissions. IC 443 is a shell-type supernova remnant and it has an angular extent of 45’ in the radio wavewband with a complex shape consisting of two half-shells with different radii.

The age of IC 443 remains uncertain, with various estimates placing it in the range ~3–40 kyr but other analyses indicate that it is older (20−30 kyr). IC 443 SNR is one of the best candidates for the investigation of the connection among SNRs, molecular clouds and high- and very high energy gamma-ray sources. Available observations suggest that IC 443 has been interacting with surrounding interstellar matter.

The close placement of the dense shocked molecular clouds and GeV−TeV gamma-ray emission regions detected by EGRET, Fermi LAT, MAGIC and VERITAS suggests that IC 443 can be considered as a candidate to the hadronic cosmic-ray source.

IC 443 SNR

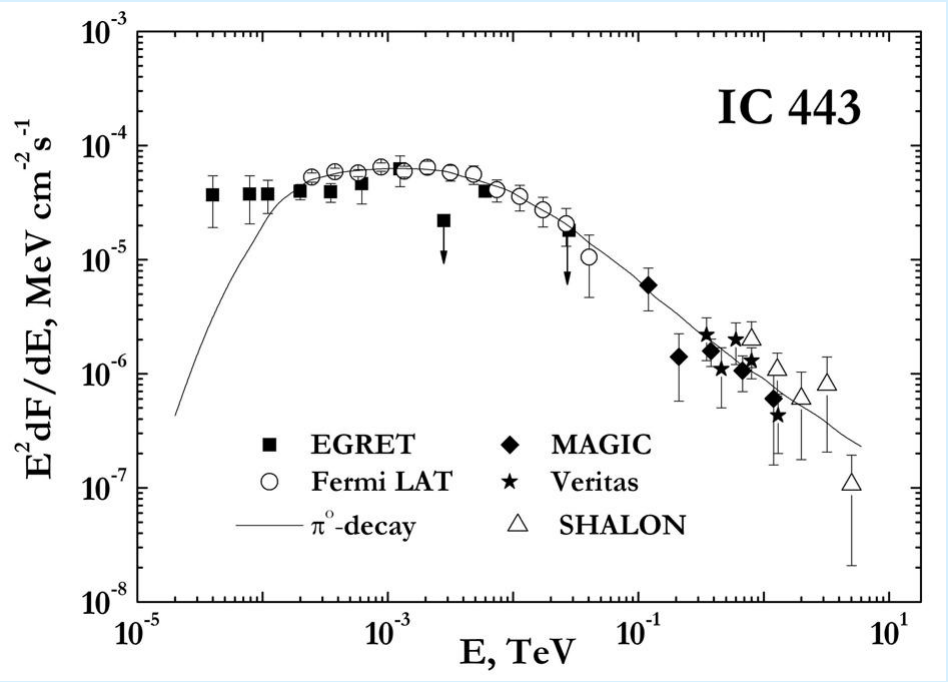

IC 443 was detected in TeV gamma-rays, first by MAGIC (2007) and later confirmed by VERITAS (2009) and SHALON (2011). The high energy gamma-ray emission from IC 443 was detected with EGRET (1995) and then with Fermi LAT (2010) in the range 500 MeV - 50 GeV.

The favored scenario in which the *gamma*-rays of 100 MeV – 4 TeV energies are emitted in the shell of the IC443 SNR is π^o-decay which produced in the interactions of the cosmic rays with the interstellar gas. Inverse Compton scattering can not explain the observed IC 443 gamma-ray emission as there is no bright source of seed photons in the region of the IC 443.

The spectral energy distribution of the *gamma*-ray emission from IC443 by SHALON (Δ) in comparison with other experiment data EGRET Fermi LAT, MAGIC, VERITAS and with theoretical predictions. Solid line shows the very high energy *gamma*-ray spectra of hadronic origin.

IC 443 was detected by SHALON with the integral flux above 0.8TeV:

$$\mathbf{I_{IC\ 443}\ (>0{,}8TeV) = (1{,}69 \pm 0{,}58) \bullet 10^{-12}\ cm^{-2}s^{-1}}$$

with a statistical significance of **7.2σ** (Li&Ma).

Crab Nebula (1054yr)

To made a description of the intensity and spectral shape in the TeV region, the model of Inverse Compton scattering of the ambient photons in the nebula in the [Hillas,1998] is used.

The TeV gamma-quantum spectrum of Crab by SHALON is generated via Inverse Compton of soft, mainly optical, photons which are produced by relativistic electrons and positrons, in the nebula region around 1.5' from the pulsar with specific average magnetic field of about 67nT.

The TeV gamma-quantum spectrum of Crab by SHALON (open triangles) in comparison with other experiments: Whipple, EGRET, CANGAROO Lines show predicted inverse Compton spectrum for four different field strengths: 10nT, 16nT, 40 nT [Hillas, 1998] and **67nT** (this work)

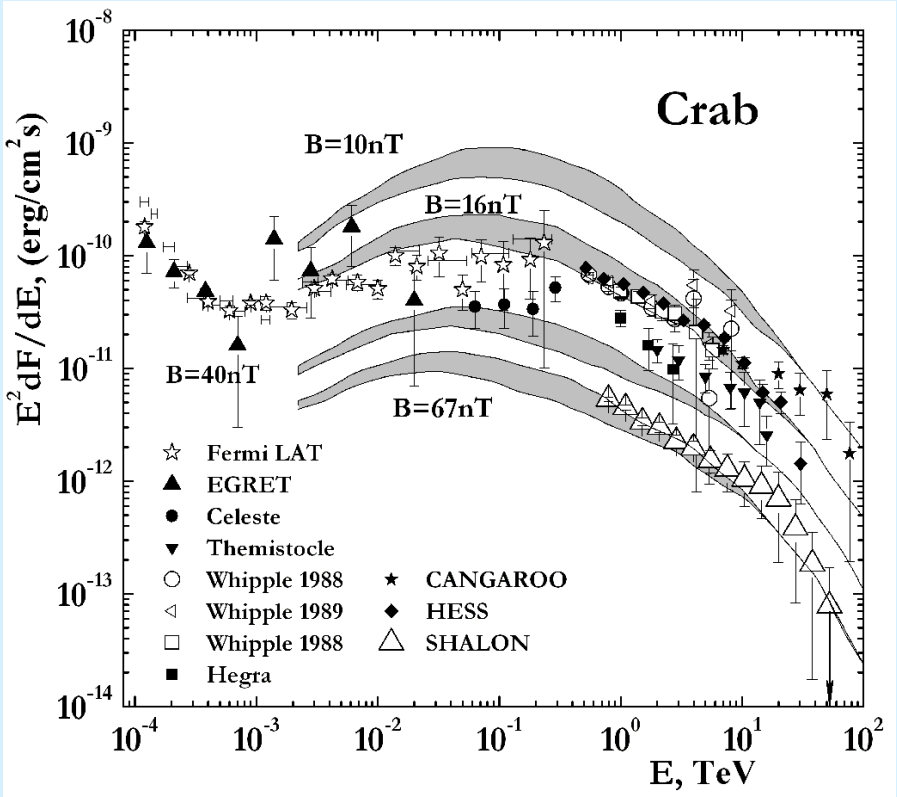

The Crab PWN in the energy range 0.2 -4.1 keV. Image of the central 200''×200'' of the Crab Nebula. In this energy band most of the PWN X-rays come from a torus surrounding the pulsar. The red contour lines show the 0.8 – 30 TeV - structure by SHALON observations. The most part of TeV energy gamma-quanta come from the region of bright torus whereas the contribution of energy gives the region of the southern jet.

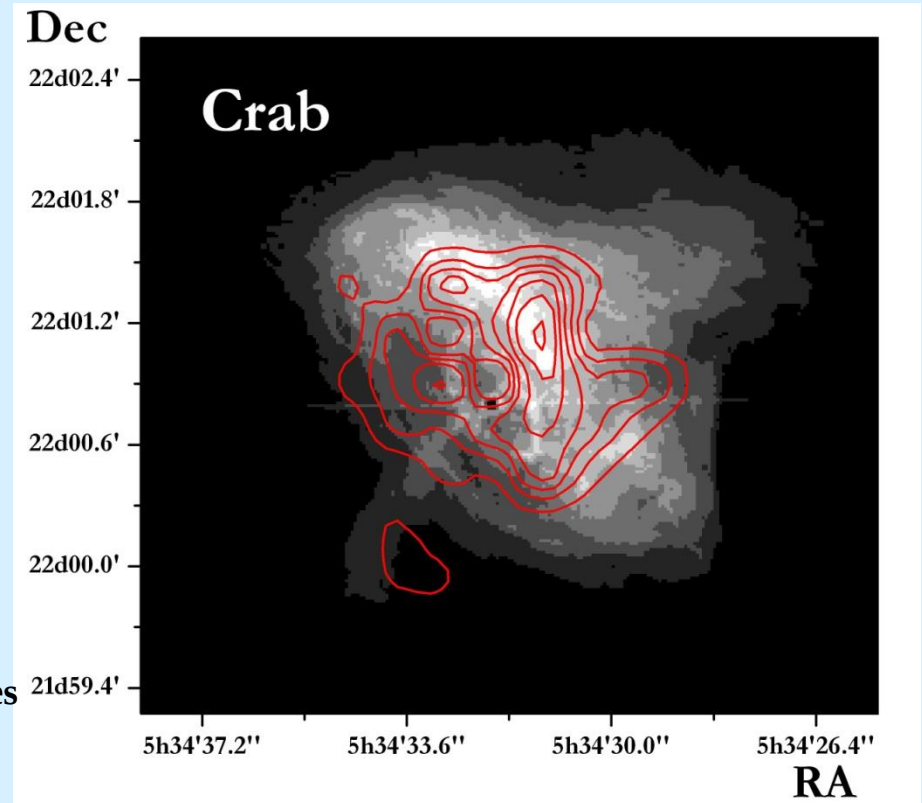

A Chandra X-ray image of Crab Nebula. The red contour lines show the 0.8 – 30 TeV - structure by SHALON observations

3c 58(SN1181) age of (2 ÷ 5)×10^3yr. or 1181y.?

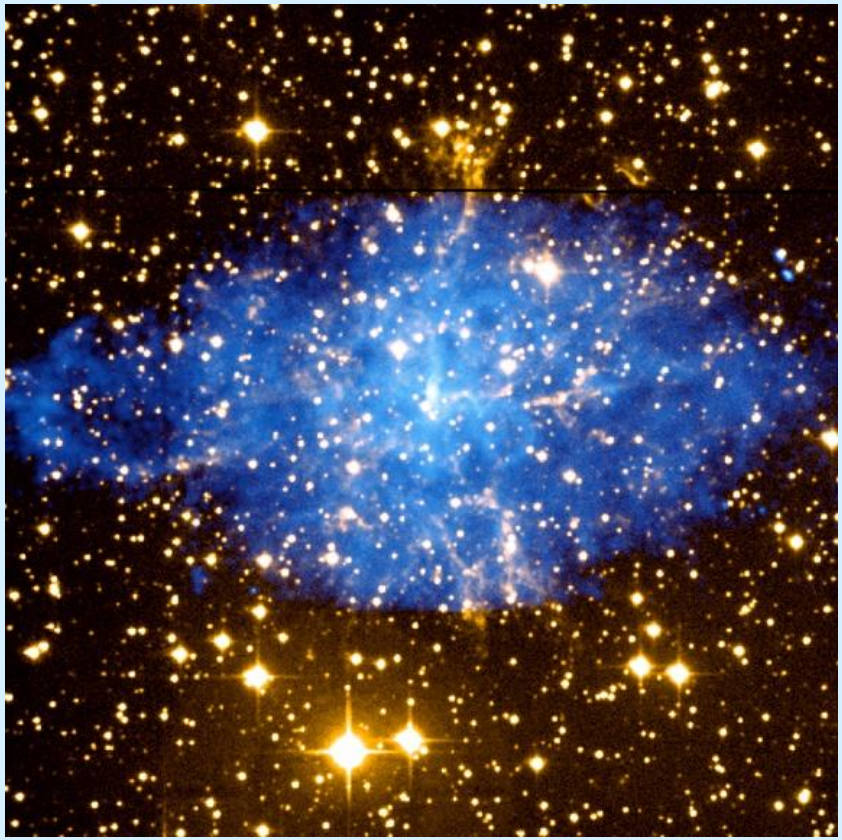

The composite image of 3c58

Optical data from the 1.3m McGraw-Hill are yellow;
X-ray data from the Chandra X-ray Observatory are blue.

The radio source 3C58 was recognized to be a supernova remnant and coincides positionally with the historical supernova SN 1181. By the structure of radio brightness distribution 3C58 is classified as a plerion (PWN) like Crab Nebula supernova remnant. Then, an X-ray point source in the center of 3C 58 was identified as a likely pulsar, and later studies yielded a distance of 3.2 kpc. The pulsar J0205+6449 was finally discovered in Chandra data in X-rays and then this was followed by the detection of weak radio pulsations from PSR J0205+6449. It supposed that these X-ray and radio data could explain the powering of the nebula. But there are a serious problems. The 3C 58/J0205+6449 system coincides positionally with the 828 yr old historical supernova SN 1181. However, both the dynamical age of the pulsar (5400 yr) determined from its spindown rates and the dynamical age of 5000±2250 yr corresponding to the mean expansion velocity of the 3C58 determined by comparing the VLA radio images in 1973 and 1998 are incompatible with the age of the remnant of SN 1181.

3c58 (SN1181)

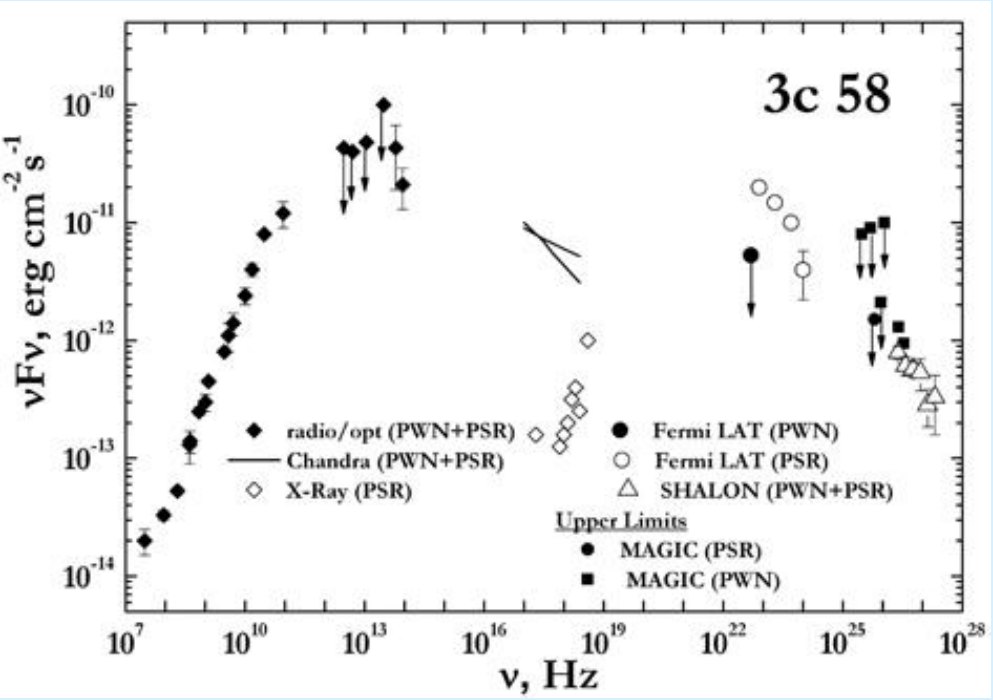

The spectral energy distribution of the *gamma*-ray emission from 3C 58 by SHALON (Δ) in comparison with other experiment data.

The observations of the very high energy γ-rays could provide an important information about the evolution of PWN from the young Crab-like to the older one.

3C 58 is similar to the Crab nebula both having a flat-spectrum radio nebula, nonthermal extended X-ray emission, and point-like X-ray emission originating from a central pulsar, but these two objects differ significantly in luminosity and in size. The radio emission of nebula of 3C 58, although ~2 times larger, is less luminous than the Crab by an order of magnitude, but its X-ray luminosity is ~2000 times smaller. These discrepancies could be explained by a different age. The observations of the very high energy γ-rays could provide an important link in the evolution of PWN from the young Crab-like stage to the older plerion stages.

3C 58 was observed by SHALON in 2011, 2012 for a total of 28.7 hours, during moonless nights at zenith angles ranging from 13° to 35°. All observations were made with the standard procedure of SHALON experiment.

After the standard analysis the *gamma*-ray source associated with the 3c 58 was detected above 800 GeV with a statistical significance of 6.8σ *(Li&Ma)*. The integral energy spectrum of 3c58 can be well described by a power law with the index -1.33±0.12. The observed integral flux of 3c 58 above 0.8TeV is

$$\mathbf{I_{3C58}(>0{,}8\ TeV) = (0{,}56\pm0{,}15)\bullet10^{-12}\ cm^{-2}s^{-1}.}$$

Cygnus X-3

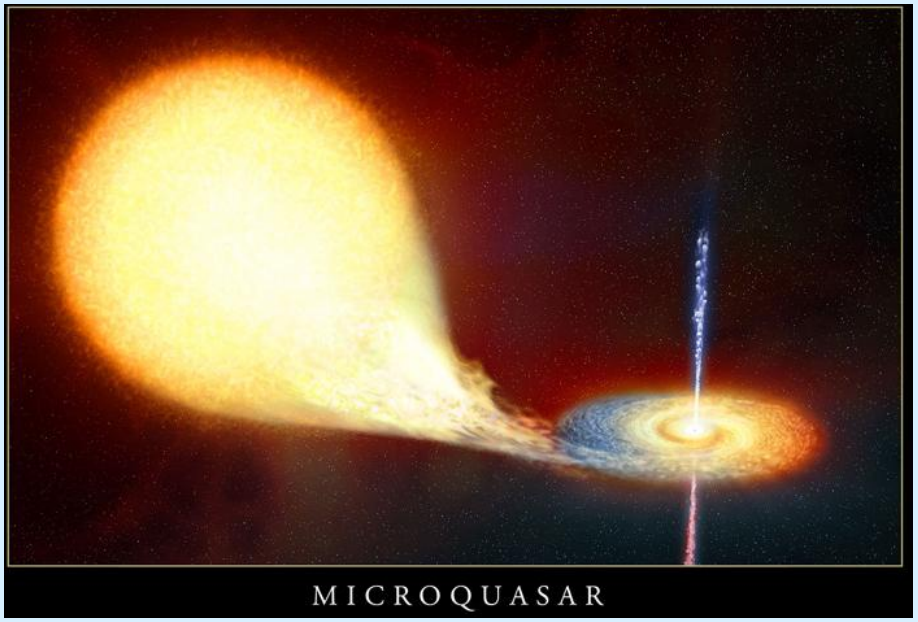

Cyg X-3 is peculiar X-ray binary system discovered about 40 years ago. The system has been observed throughout wide range of the electromagnetic spectrum. It is one of the brightest Galactic X-ray sources, displaying high and low states and rapid variability in X-rays. It is also the strongest radio source among X-ray binaries and shows both huge radio outbursts and relativistic jets. The radioactivity is closely linked with the X-ray emission and the different X-ray states. Based on the detections of ultra high energy gamma-rays, Cygnus X-3 has been proposed to be one of the most powerful sources of charged cosmic ray particles in the Galaxy.

The spectral energy distribution of Cyg X-3. Black points are the archival data from Cordova, (1986). The high level points in radio and X-ray bands correspond to radio-frequency activity and increased x-ray activity of the source. TeV range is represented with integral spectrum by SHALON (Δ data-1995 – 2013yy) in comparison with other experiments: TIBET, HEGRA, EAS-TOP, Whipple, CASA-MIA, Kiel, Havera Park

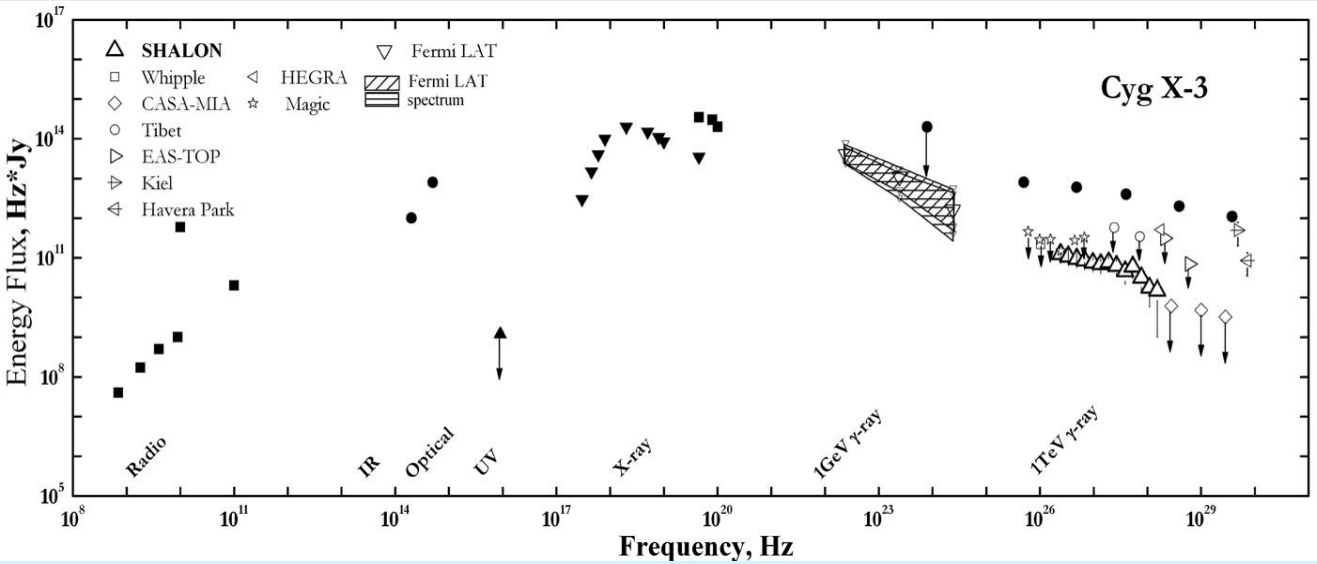

Cygnus X-3

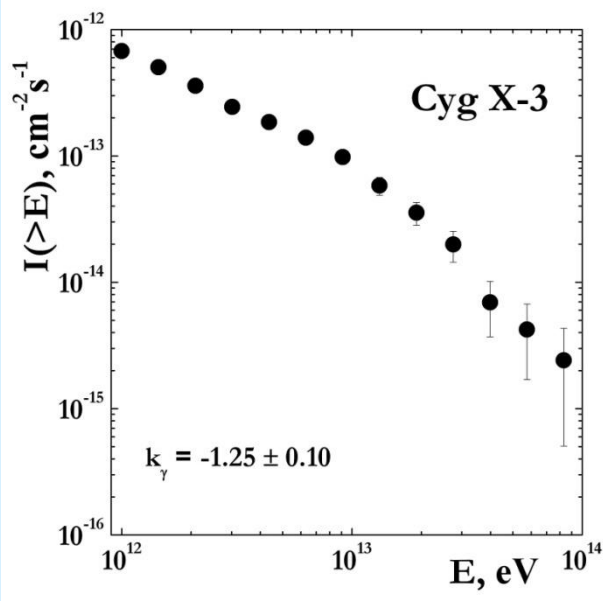

Cyg X-3 has been regularly observed since a 1995 with SHALON telescope during the 246 hours in total. All observations were made with the standard procedure of SHALON experiment during moonless nights with zenith angles from 4 to 35 degree. The gamma-ray source associated with the Cyg X-3 was detected above 800 GeV with a statistical significance of **29.8σ** Li&Ma with a γ-ray flux above 800 GeV :

$$\mathbf{F(E_O>0{,}8\ TeV)=(6.8\pm0.5)\bullet10^{-13}\ cm^{-2}s^{-1}}$$

The energy spectrum of Cyg X-3 at 800 GeV - 85 TeV can be approximated by the power law $F(>E_O) \propto E^{k\gamma}$, with k_γ=-1.25± 0.10. This flux, measured for the first time, is several times less than the upper limits established in the earlier observations.

For example, the images of Cyg X-3 in silent period at 2005 and flaring period of 1997y are shown in comparison. There are no features revealed at flaring periods found at 2005y. The last two significant increase of very high energy gamma-quantum flux have detected in May 2009 and October 2011, which is correlated with flaring activity at lower energy range of X-ray and/or at observations of Fermi LAT. Earlier, in 1997, 2003 and 2006 a comparable increase of the flux over the average value was also observed

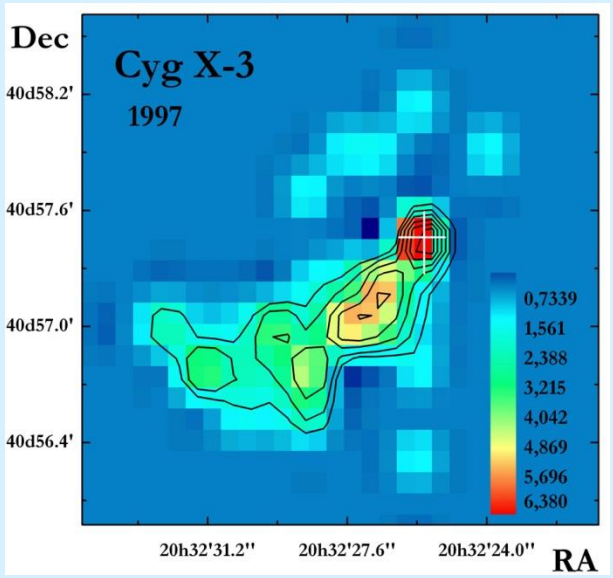

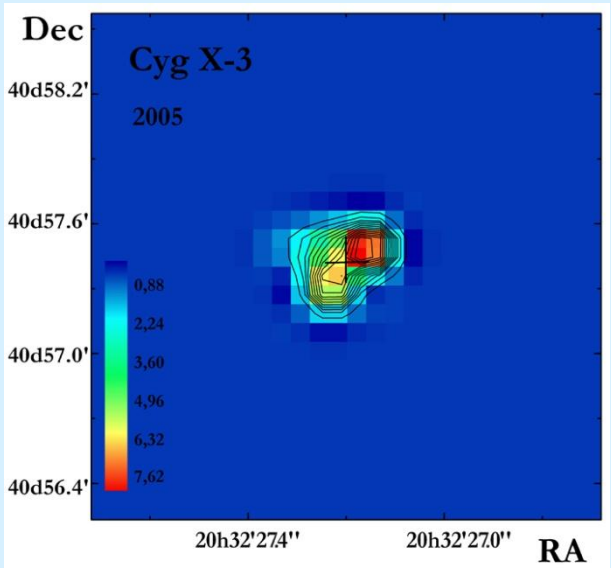

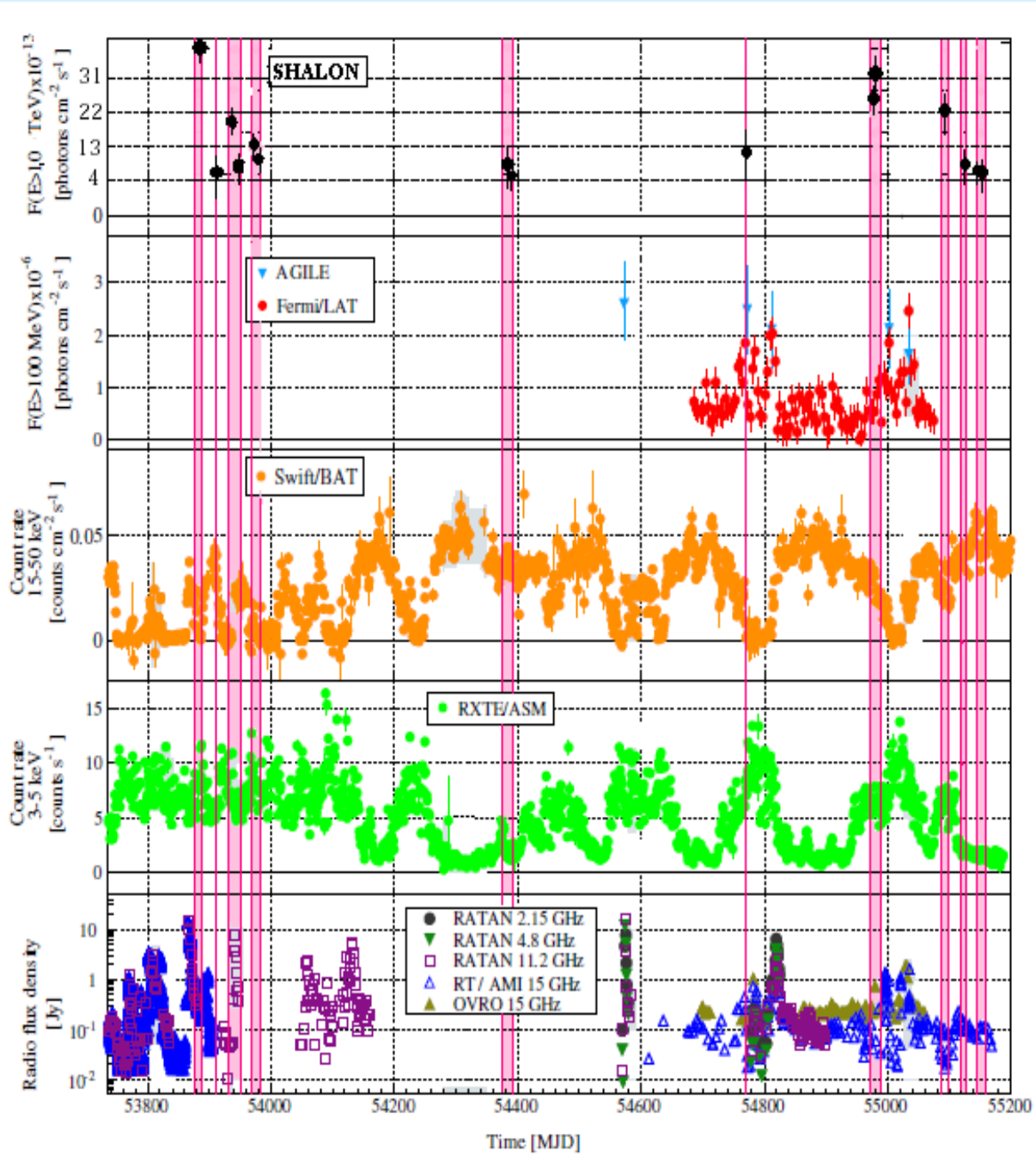

During the period of observations of Cyg X-3 with SHALON 8 significant flux increases were detected at energies above 0.8 TeV. To reveal possible correlation of periods of activity in the TeV energy range with the fairings at the low energies the light curves of Swift/BAT (15 - 50keV),35 RXTE/ASM (3 - 5 keV), 35 the fluxes at radio-ranges from RATAN, RT/AMI, OVRO35 and TeV fluxes from SHALON observations were analyzed.

The significant anticorrelation of the fluxes at TeV and hard X-rays and the correlation of very high energy flux and soft X-ray were found. It is note, that TeV flaring activities occur close (within the 4 – 5 days) to strong radio flares. Probably, it is linked with the powerful ejection from the regions are close to the centers blackhole. This ejection is accompanied with a relativistic shock where the relativistic electrons and magnetic field are generated e®ectively. Similar relation of TeV and soft X-ray fluxes were found in the 1997 observation period. But the flux increase of 2003 didn't obey this scheme, it was in the quite period in the soft X-rays. In general, the correlation soft X-ray and very high energy *gamma*-ray fluxes is traced since 1996.

γ Cygni SNR age of 5000 – 7000yr.

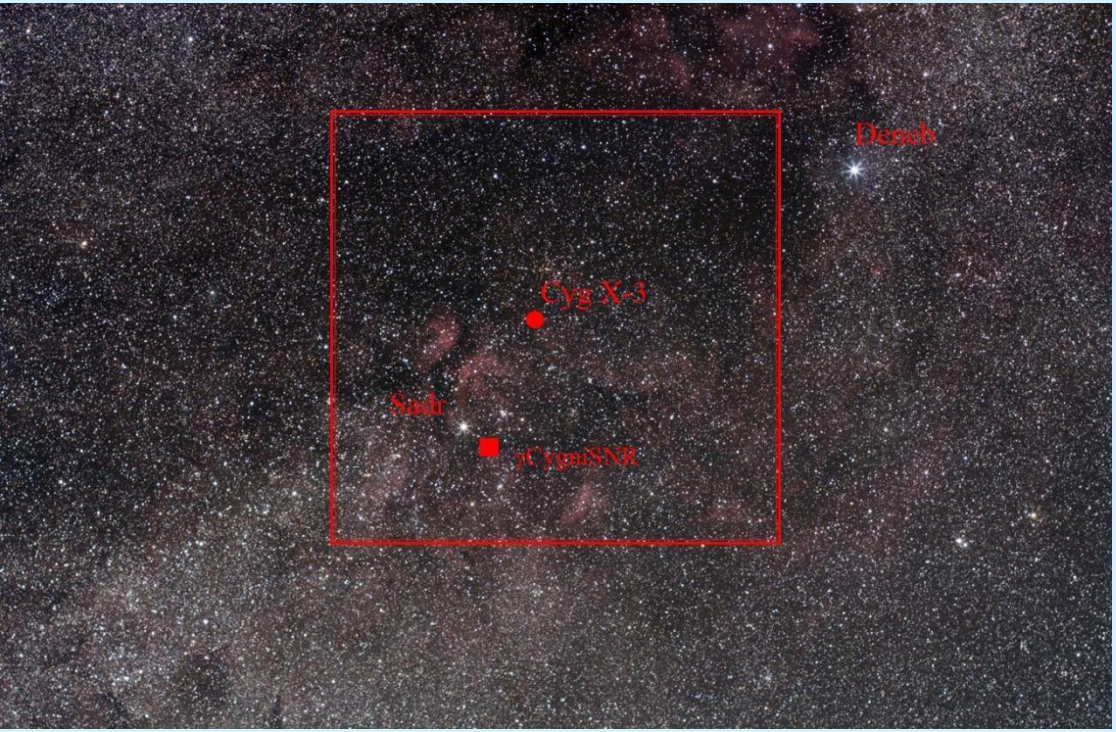

During the observations of Cyg X-3 the SHALON field of view contains γCygni SNR as it located in Cygnus Region at ~2° SW from Cyg X-3. So due to the large telescopic field of view (~8°) the observations of Cyg X-3 is naturally followed by the observations (tracing) of γCygni SNR.

SHALON telescope field of view during the observation of Cyg X-3

γCygni SNR as a source accompanying to Cyg X-3 is systematically studied with SHALON telescope since 1995y. γCygni SNR was observed with SHALON telescope during the period from 1995 till now for a total of 240 hours. The γ-ray source associated with the γCygni SNR was detected above 800 GeV with average gamma-ray flux above 0.8 TeV:

$$\mathbf{I_{\gamma Cygni\ SNR}(>0{,}8TeV) = (1{,}27\pm0{,}11)\bullet10^{-12}\ cm^{-2}s^{-1}}$$

with a statistical significance of **14σ** *Li&Ma*.

[V.G. Sinitsyna**,** V.Y. Sinitsyna, 2013, Bull. of the Lebedev Physics Institute, v. 40(5), pp. 113 – 118]

γ Cygni SNR

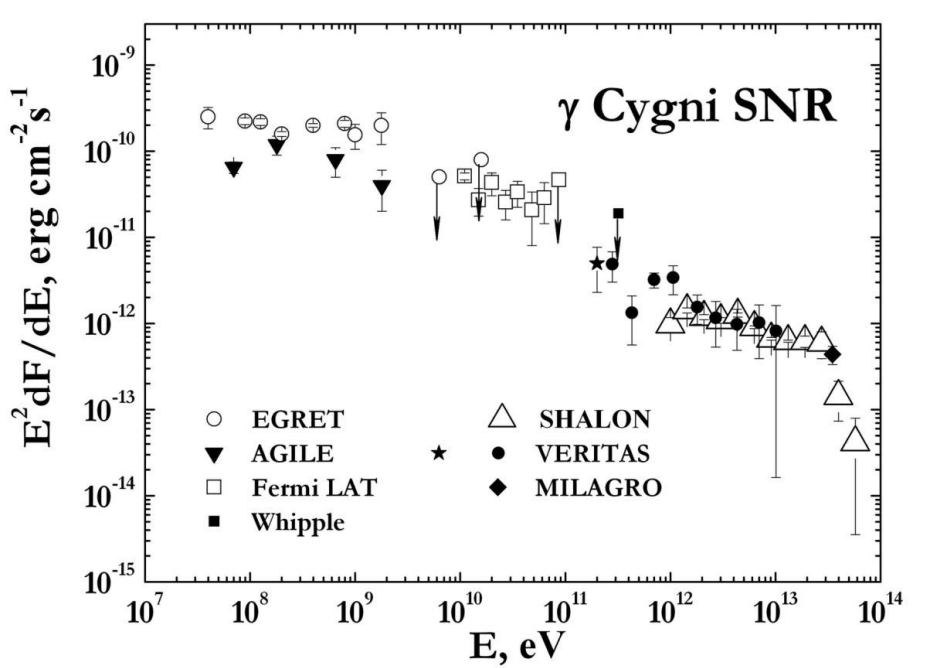

The energy spectrum of γ-rays in the observed energy region from 800GeV to 50 TeV is well described by the power law with exponential cutoff:

$$I(>E_\gamma/TeV)=(1{,}12\pm0.11)\times(E_\gamma/(1TeV))^{-0{,}93\pm0{,}09}\exp(-E_\gamma/20TeV)$$

The spectral energy distribution of the *gamma*-ray emission from γCygni SNR by SHALON (Δ) in comparison with other experiment data EGRET, AGILE, Fermi LAT, Whipple, VERITAS, MILAGRO.

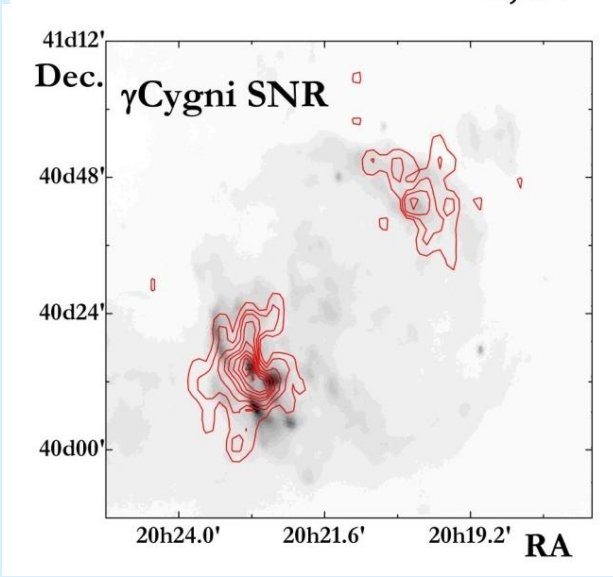

Radio image of γCygni SNR (CGPS); The contour lines show the TeV-image by SHALON

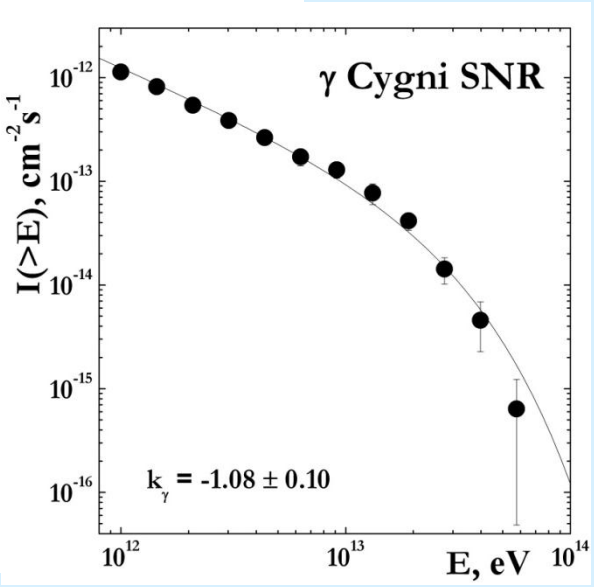

The *γ*-ray integral spectrum by SHALON at energies 0.8 – 28 TeV is compatible with a power law: $I(>E_\gamma)\propto E_\gamma^{-1{,}08\pm0{,}10}$

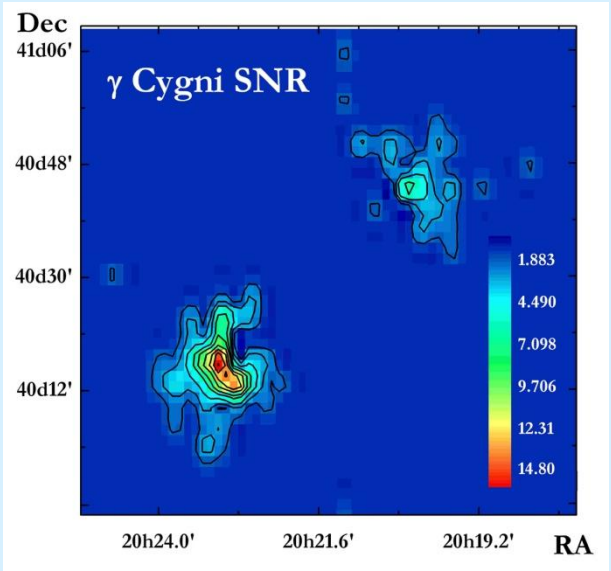

The image of γCygni SNR by SHALON

TeV GAMMA-RAY EMISSION from METAGALACTIC SOURCES

The gamma-astronomical researches are carrying out with SHALON mirror telescope at the Tien-Shan high-mountain observatory. During the period 1992 - 2014, SHALON has been used for observations of the metagalactic sources Mkn421, Mkn501, NGC1275, OJ 287, 3c454.3, 1739+522 and galactic sources Crab Nebula, Cygnus X-3, Tycho's SNR, Geminga, 2129+47XR.

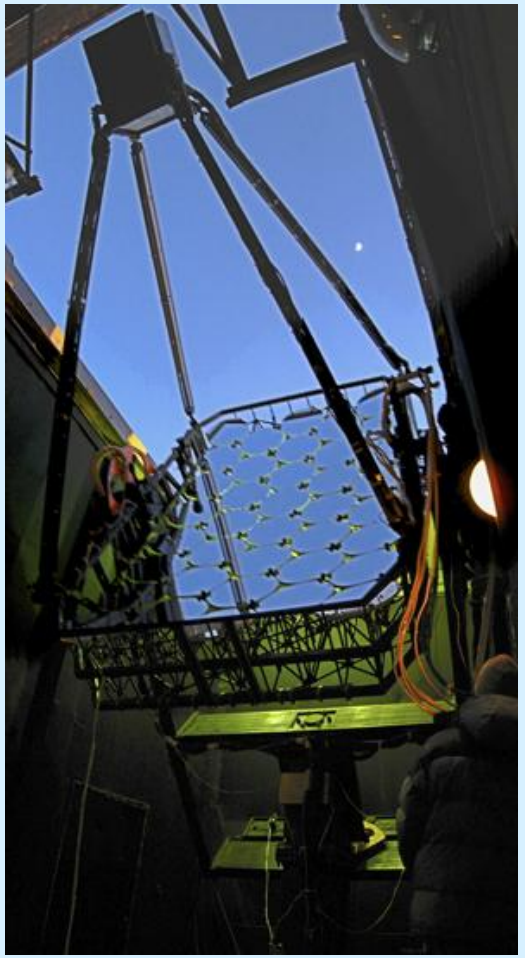

SHALON catalogue of metagalactic γ -quantum sources

Source	Observable flux, $cm^{-2}s^{-1}$	z	Source type
NGC 1275	$(0.78\pm0.05)\times10^{-12}$	0.0179	Syefer Galaxy
SN2006 gy	$(3.71\pm0.65)\times10^{-12}$	0.019	Extragalactic Supernova
Mkn 421	$(0.63\pm0.05)\times10^{-12}$	0.031	BLLac
Mkn 501	$(0.86\pm0.06)\times10^{-12}$	0.034	BLLac
Mkn 180	$(0.65\pm0.09)\times10^{-12}$	0.046	BLLac
3c382	$(0.95\pm0.33)\times10^{-12}$	0.0579	Radio Galaxy
4c+31.63	$(0.72\pm0.22)\times10^{-12}$	0.295	FSRQ
OJ 287	$(0.26\pm0.07)\times10^{-12}$	0.306	BLLac
3c4543	$(0.43\pm0.07)\times10^{-12}$	0.859	FSRQ
4c+55.17	$(0.68\pm0.17)\times10^{-12}$	0.896	FSRQ
1739+522	$(0.53\pm0.05)\times10^{-12}$	1.375	FSRQ

NGC 1275

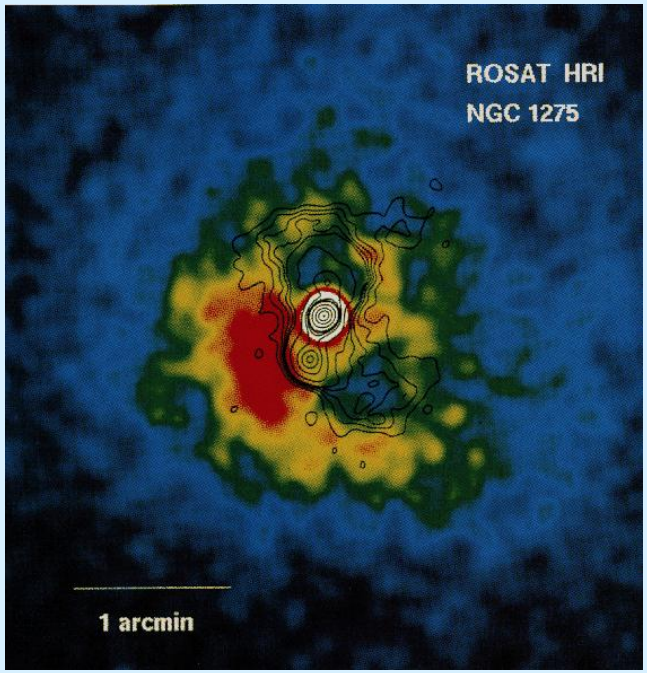

The cluster of galaxies in Perseus is one of the best-studied clusters due to its relative proximity (its distance ~100 Mpc or redshift z = 0.0179) and brightness. Clusters of galaxies have long been considered as possible candidates for the sources of TeV gamma rays emitted by protons and electrons accelerated at large-scale shocks or by a galactic wind or active galactic nuclei. NGC 1275 is a powerful source of radio and X-ray emission. In the radio band, the object found in NGC 1275, has a powerful and compact core that has been well studied with VLBI. NGC 1275 is extremely bright in the radio band; its structure consists of a compact central source and an extended jet. The galaxy NGC 1275 historically aroused great interest due to both its position at the center of the Perseus cluster and its possible "feedback" role.

A ROSAT HRI image of the region around the galaxy NGC 1275 at the centre of the Perseus galaxy cluster. The contour lines show the radio structure as given by VLA observations. The maxima of the X-ray and radio emission coincide with the active nucleus of NGC 1275. In contrast, the X-ray emission disappears almost completely in the vicinity of the radio lobes.

Long-term studies of the central galaxy in the cluster, NGC 1275, are being carried out in the SHALON experiment. We presented the results of fifteen-year-long observations of the AGN NGC 1275 at energies 800 GeV–40 TeV discovered by the SHALON telescope in 1996 with integral flux $\mathbf{(0.78\pm0.05)\times10^{-12}cm^{-2}s^{-1}}$. The energy spectrum of NGC 1275 at >0.8 TeV can be approximated by the power law $F(>E_O) \propto E^{k\gamma}$, with $k\gamma$ = -2.24 ± 0.09. Gamma-ray emission from NGC 1275 was detected by the SHALON telescope at energies above 800 GeV at the **31.4σ** confidence level determined according to Li and Ma .

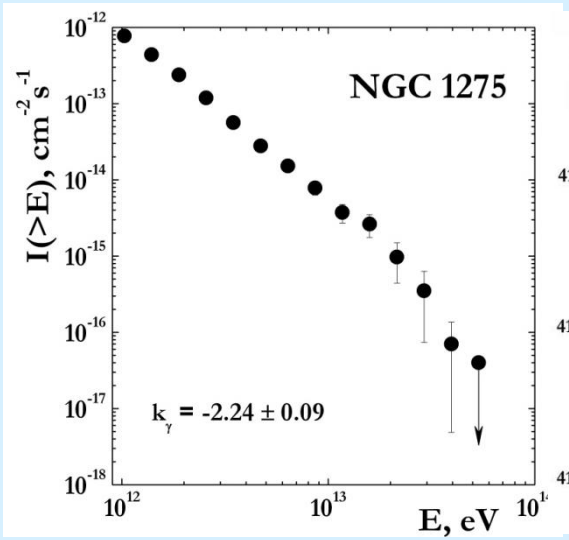

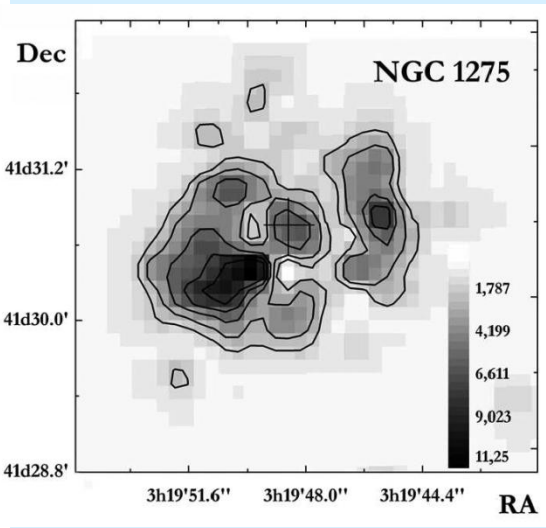

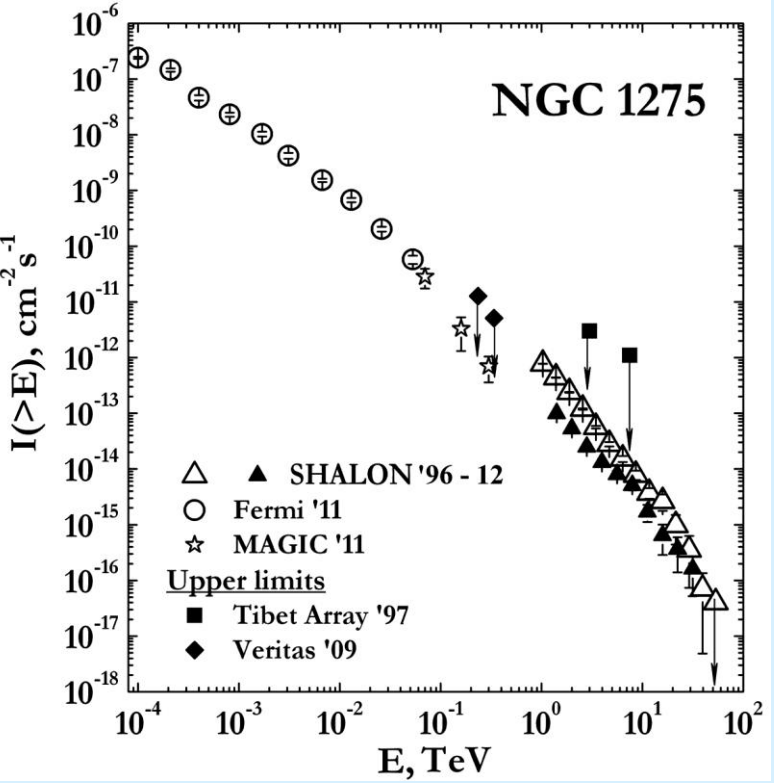

NGC 1275

To analyze the emission related to this core, we additionally identified the emission component corresponding to the central region of NGC 1275 with a size of 32”. The emission from the central region of NGC 1275 was detected at energies above 0.8 TeV at a 13.5σ confidence level determined by the Li&Ma method with a average integral flux:

$$I(>800\ \text{GeV}) = (3.26\pm0.3)\times10^{-13}\ \text{cm}^{-2}\text{s}^{-1}.$$

The gamma-ray energy spectrum of the central component in the entire energy range from 0.8 to 40 TeV is well described by a power law with an exponential cutoff,

$$I(>E_\gamma)=(2.92\pm0.11)\times10^{-13}\times E_\gamma^{-1.55\pm0.10}\times\exp(-E_\gamma/10\text{TeV})\text{cm}^{-2}\text{s}^{-1}$$

The integral gamma-ray spectrum of NGC1275 and its central region obtained from SHALON data (1996–2012) with the Fermi LAT (2009–2011) and MAGIC (2010–2011) experimental data.

The SHALON spectrum corresponding to the emission from the central region of NGC 1275 is represented by the black triangles

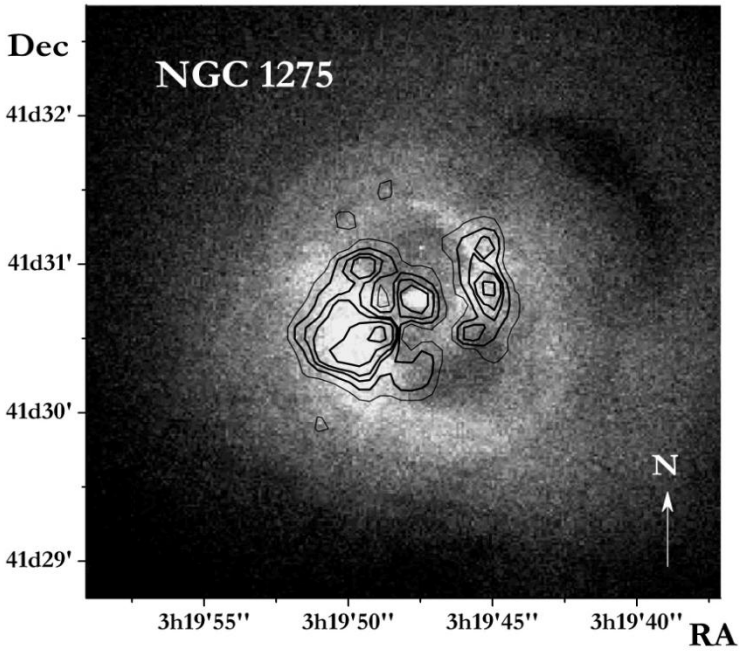

NGC 1275

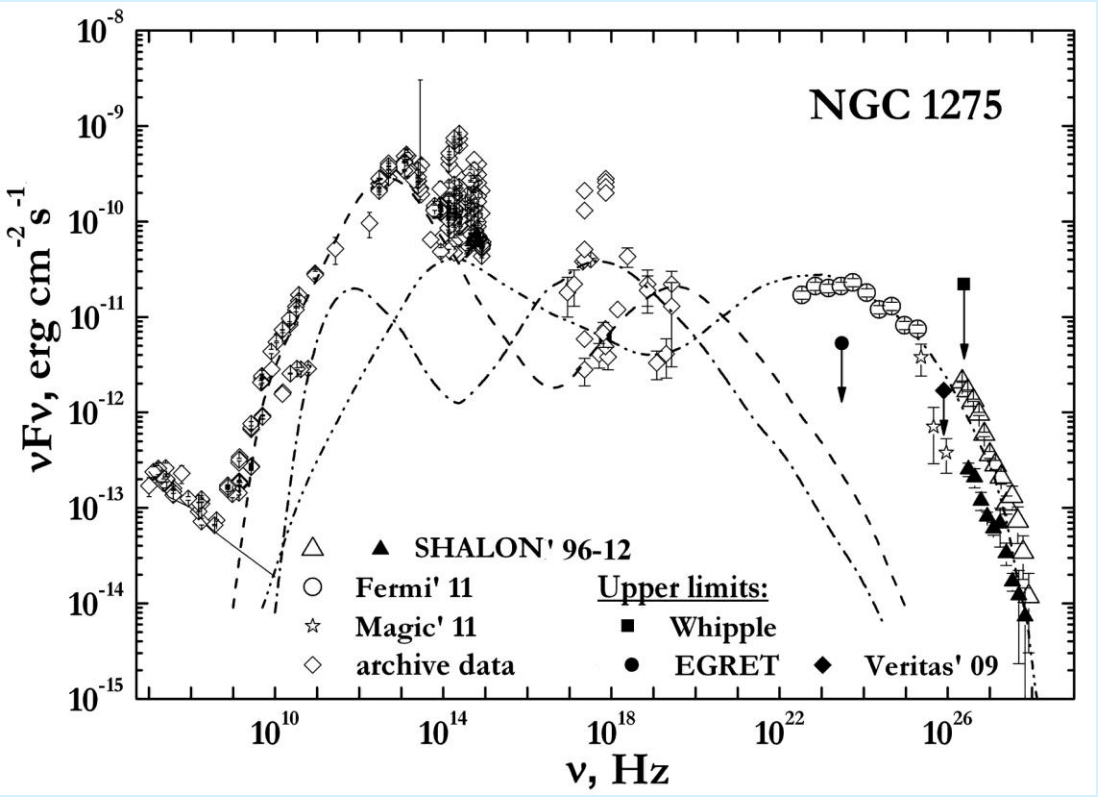

The multifrequency spectral energy distribution for the nucleus of NGC 1275, up to high and very high energies, was described in the CM model (Colafrancesco et al. 2010) and is a composition of the components of inverse Compton scattering of the intrinsic synchrotron radiation from relativistic electrons (synchrotron self-Compton) of three separate plasma blobs ejected from the inner regions of the NGC 1275 nucleus (the dashed, dash–dotted, and dash–dotted with two dots curves).

Overall spectral energy distribution of NGC 1275. The TeV energy spectrum of NGC 1275 from SHALON, 15 year observations in comparison with other experiments: Fermi LAT'09-11, MAGIC'10-11 and upper limits: EGRET'95 , Whipple'06, Veritas'09 and models.

The available Fermi LAT data at high energies and the SHALON observations at very high energies in a region < 32" around NGC1275 are described in terms of this model with one of the components produce synchrotron self-Compton emission of the relativistic jets from the nucleus itself (the dash–dotted with two dots curve).

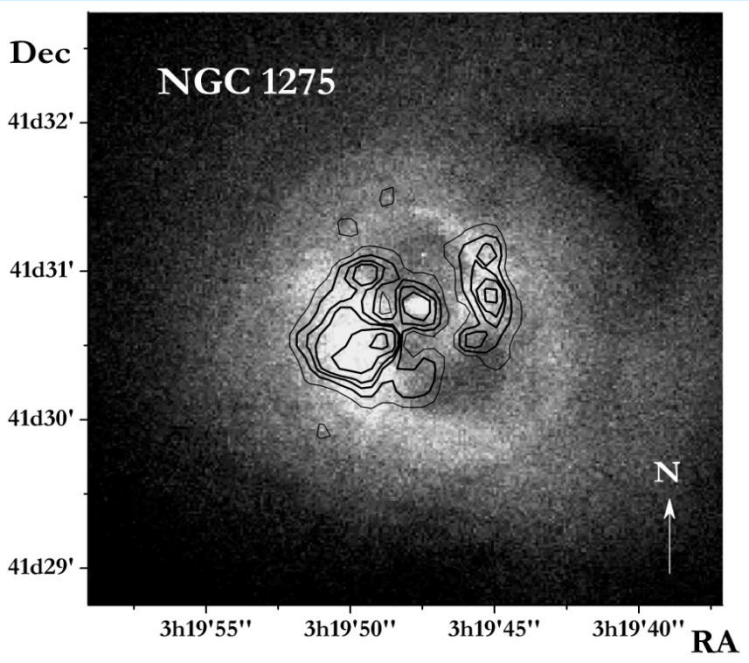

Perseus Cluster and NGC 1275

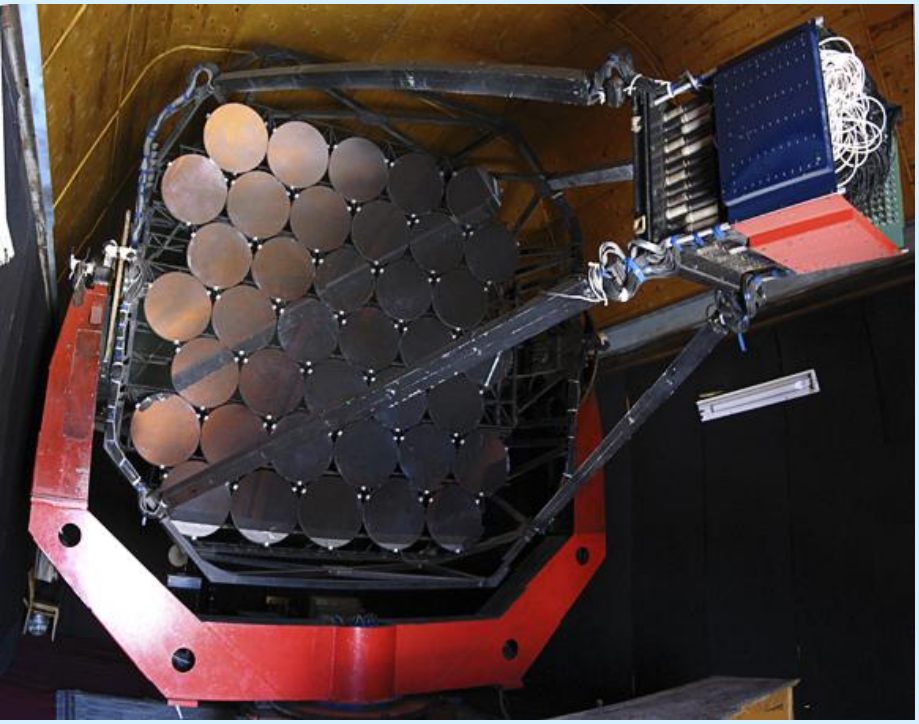

The cluster of galaxies in Perseus, along with other clusters, have long been considered as possible candidates for the sources of high and very high energy gamma-ray emission generated by various mechanisms. Long-term studies of the central galaxy in the cluster, NGC 1275, are being carried out in the SHALON experiment. We presented the results of fifteen-year-long observations of the AGN NGC 1275 at energies 800 GeV–40 TeV discovered by the SHALON telescope in 1996. **The data obtained at very high energies, namely the images of the galaxy and its surroundings, and the flux variability indicate that the TeV gamma-ray emission is generated by a number of processes: in particular, part of this emission is generated by relativistic jets in the nucleus of NGC 1275 itself. Whereas, the presence of an extended structure around NGC 1275 is evidence of the interaction of cosmic rays and magnetic fields generated in the jets at the galactic center with the gas of the Perseus cluster.**

SHALON observations of Active Galactic Nuclei

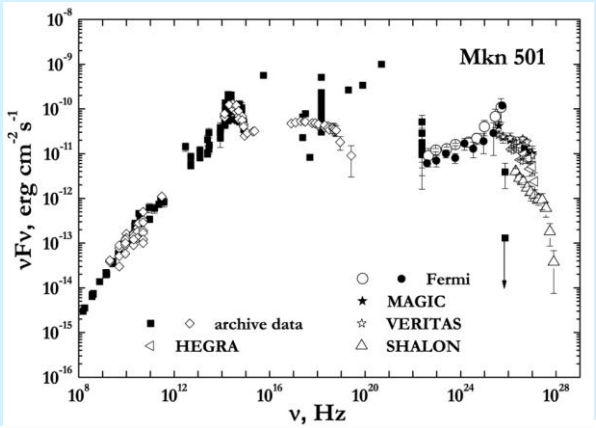

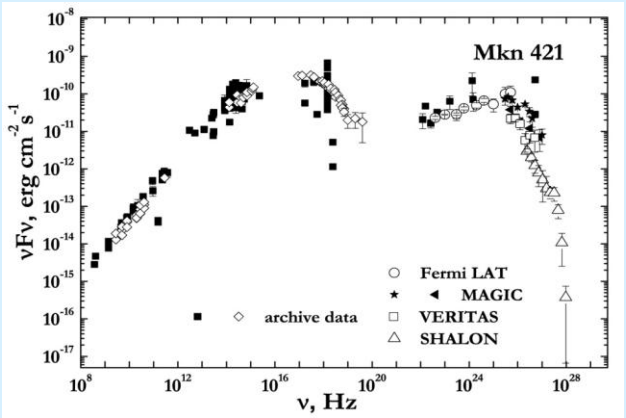

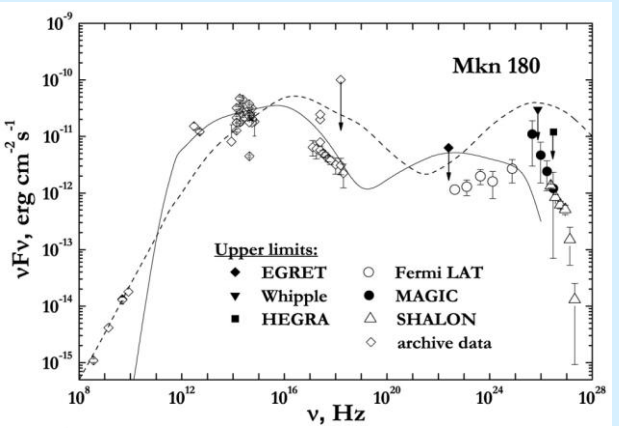

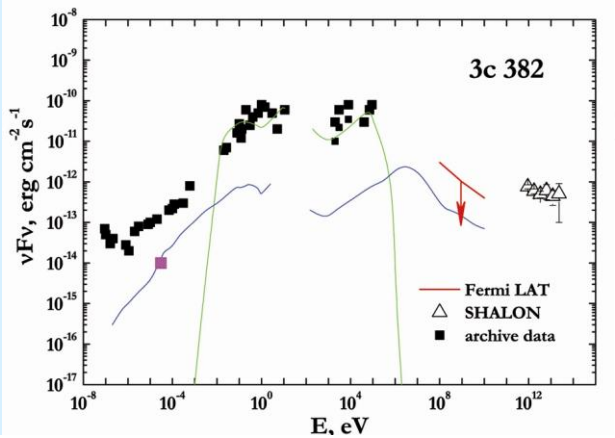

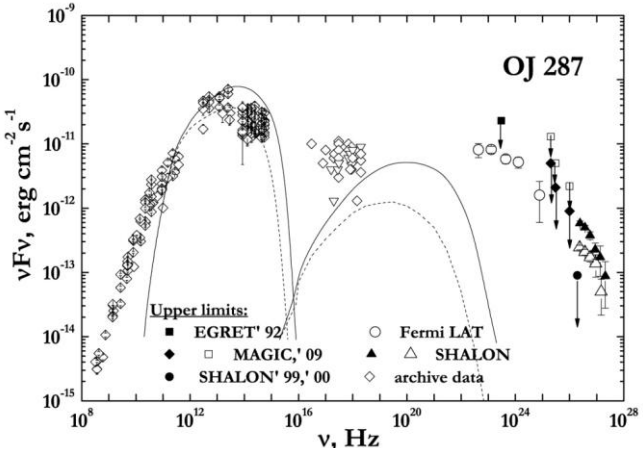

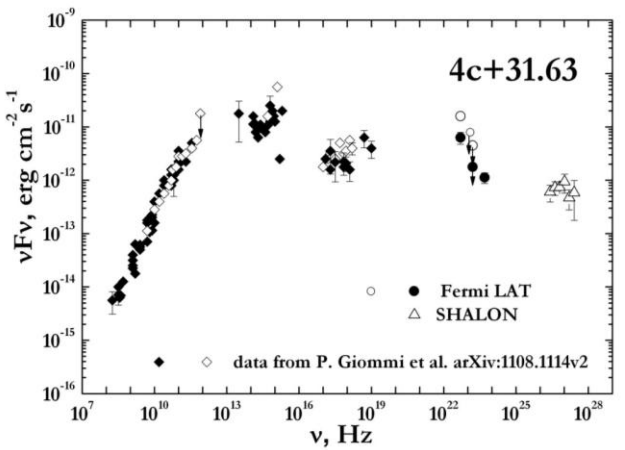

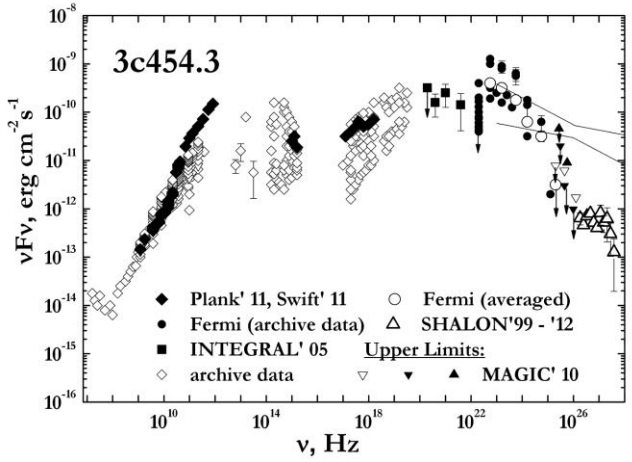

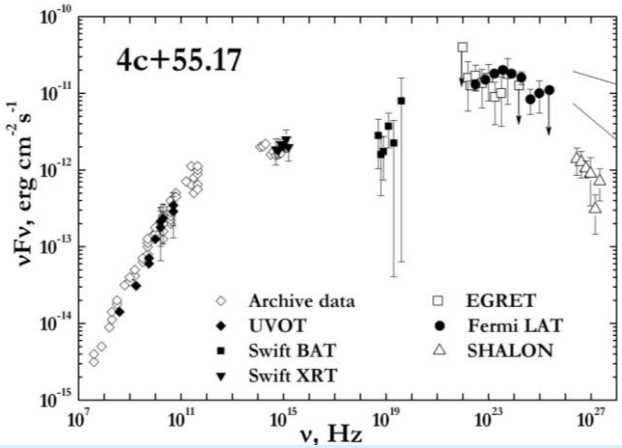

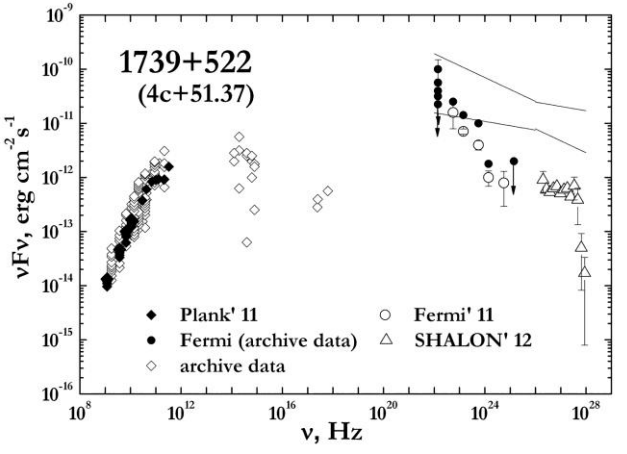

Metagalactic sources of very high energy gamma-quanta

Observations of active galactic nuclei can also be used for the study of Extragalactic Background Light. The light emitted from all objects in the Universe such as stars, galaxies, hot dust etc. during its entire history forms a background light of photons named "diffuse extragalactic background light" (EBL). The EBL spectrum contains an information about star and galaxy formation on early stages of Universe evolution. TeV gamma-rays, radiated by distant sources, mostly interact with IR-photon background via $\gamma+\gamma \rightarrow e^+e^-$ resonant process, then relativistic electrons can radiate gamma-ray with energies less than of primary gamma-quantum. As a result, primary spectrum of gamma-source is changed, depending on spectrum of background light. So, a hard spectra of Active Galactic Nuclei with high red shifts of 1.6 -1.8 allow to determine an absorption by Extragalactic Background Light and thus spectrum of EBL.

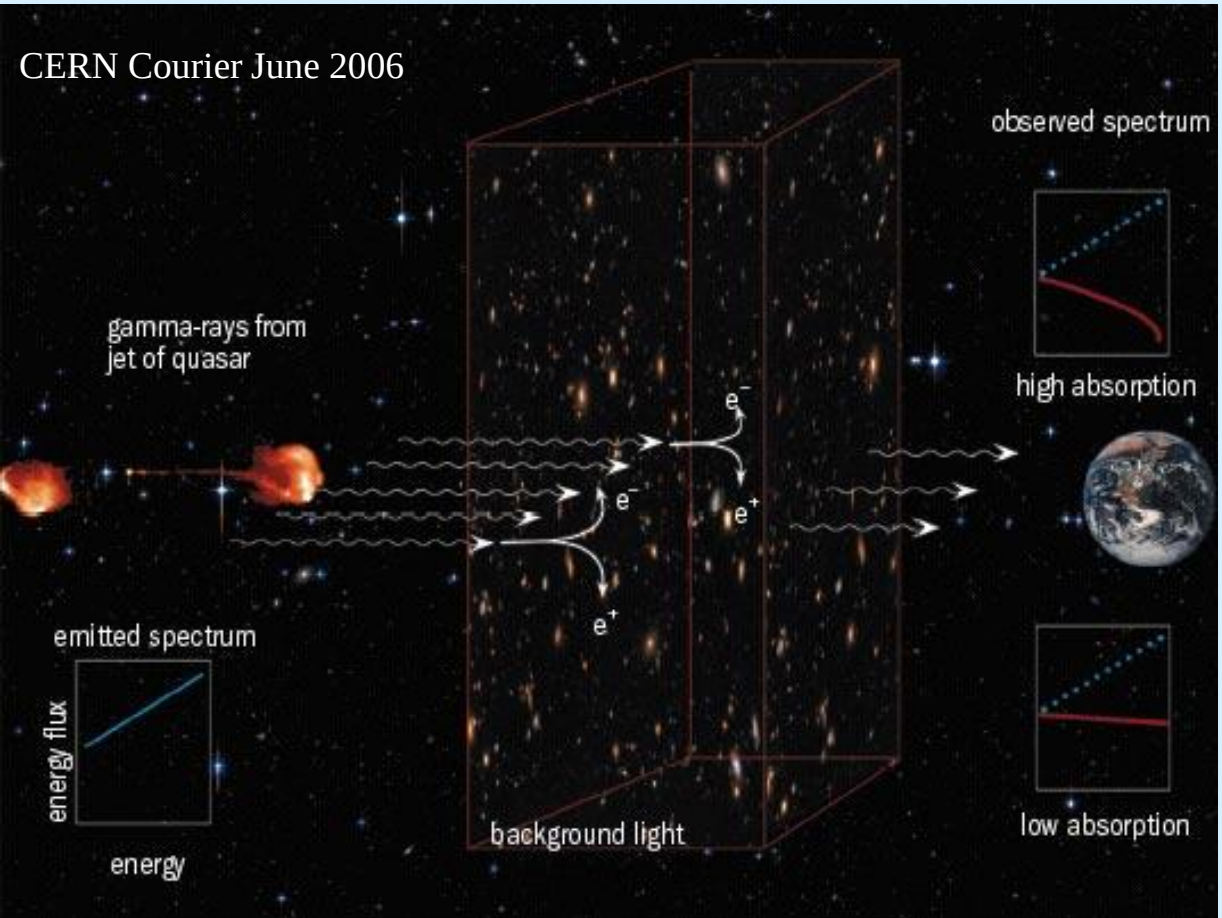

During the period 1992-2014 eleven metagalactic sources have been observed:

NGC 1275	**z = 0.0179;**
SN 2006gy	**z = 0.019;**
Mkn 421	**z = 0.031;**
Mkn 501	**z = 0.034;**
Mkn 180	**z = 0.046;**
3c382	**z = 0.0578;**
4c+31.63	**z = 0.295**
OJ 287	**z = 0.306;**
3c454.3	**z = 0.859;**
4c+55.17	**z = 0.896**
1739+522	**z = 1.375;**

Observations of distant metagalactic sources have shown that the Universe is more transparent to very high energy gamma-rays than previously believed.

Extragalactic Background Light

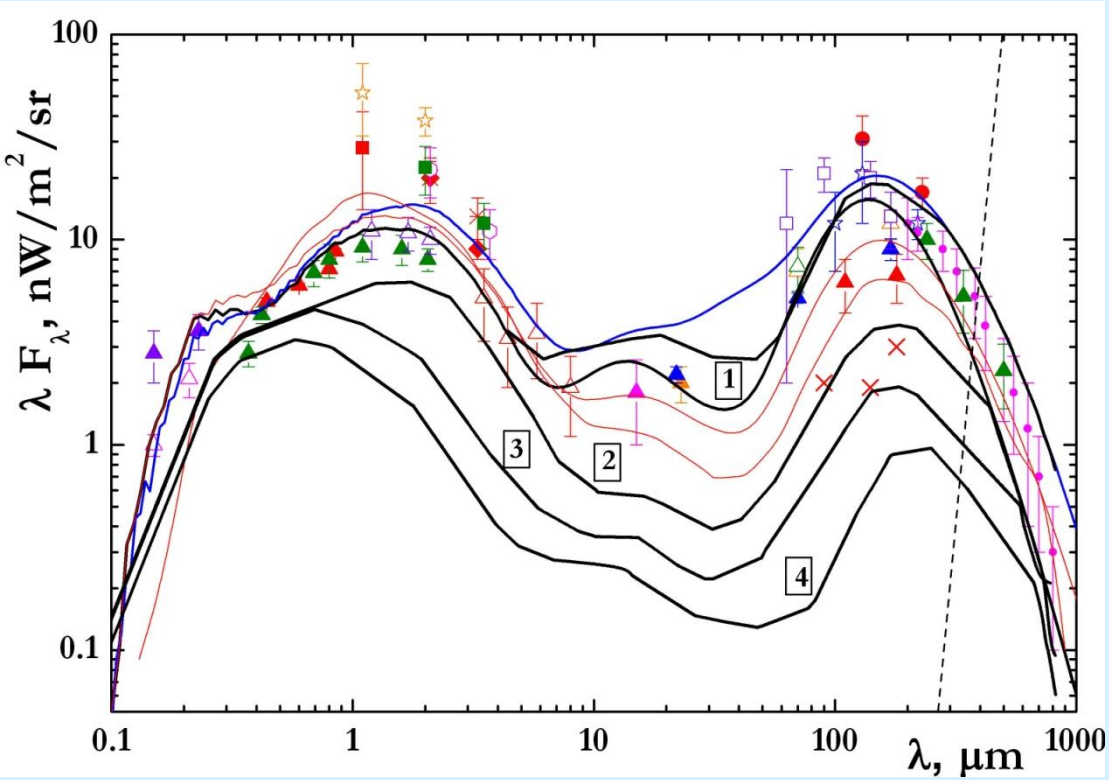

Spectral energy distribution of EBL: measurements [R.C. Gilmore, et al., ArXiv:1104.0671] and models [Stecker et. al, 2006, Kneiske et. al 2004], and EBL shape constrained from observations of the extragalactic sources by SHALON:

1 – NGC1275, Mkn421, Mkn501 and Mkn180; (averaged EBL shape from best-fit model and Low-SFR model)
2 – OJ 287 (z=0.306);
3 – 3c454.3 (z=0.859),
4c+55.17 (z=0.896);
4 – 1739+522 (z=1.375).

The detection of the very high energy gamma-ray sources at the redshifts z=0.0179 to z=1.375 with SHALON telescope gives an opportunity to constrain EBL density, based on modification to gamma-ray spectra and thus it will help to reconstruct the cosmological history of the EBL.

The detection of TeV gamma-ray sources at high red-shifts is the evidence of less average spectral density of Extragalactic Background Light and thus the less star formation rate at early evolution stage, than it is previously believed. Also, the possible explanation of the detected very high energy gamma-emission from the distant AGNi is the re-scattering of primary TeV-photons on the Dark Matter particles, so called WISP – weakly interacting slim particles. The axion-like particles has been considered to be a candidate for such weakly interacting slim particles.

A search for upward $10^{13} – 10^{16}$ eV neutrinos with SHALON atmospheric Cherenkov telescope

A neutrino telescope detects the Cherenkov radiation generated in water or ice by passage of relativistic charged particles produced by neutrino collisions with nucleons in the detector volume. Because of weakness of neutrino interaction the very large detector volume is required. Some alternative approaches have been proposed. One of them is using a earth matter or mountain as a target volume for conversion neutrinos to leptons which then initiate extensive air shower (EAS) in the atmosphere, then showers can be detected by Cherenkov telescope.

During 350 hours of observations at 97^o zenith angle after a cut of shower-like events that may be caused by chaotic sky flashes or reflections on the snow of vertical showers, we have detected 5 air showers of TeV energies. These showers have energy in the range of about 6 - 17,5 TeV. These 5 events have form characteristics and parameters similar (within 10% error) to those observed at 0^o zenith angle**.** These cascades look like the usual extensive air showers generated in atmosphere with narrow light shape. The background for this events can be some reflections of cosmic ray EAS in the mountain slope. But, first of all it could be a reflection of showers initiated by particles born in interaction of very high energy cosmic rays and rock matter nucleons. The energy of detected showers is more than 6 TeV. There is no albedo particles of such high energies. The reflection from snow which can mimed the EAS shape is excluded due to the irregular and woody structure of opposite slope (in addition: there is no snow there till the start of November). One more source of particles with high transverse energy is jet production. The probability of hadronic jet production with energy of observed showers is ten orders of magnitude less than one for detection of shower generated by secondary particles of UHE neutrino interaction.

These events may be caused by the decay of a long-lived penetrating particle entering the atmosphere from the ground and decaying in front of the telescope. As a possible explanation, we discuss two scenarios with an unstable neutrino of mass $m \approx 0.5$ GeV and $c\tau \approx 30$ m. Remarkably, one of these models has been recently proposed to explain an excess of electron-like neutrino events at MiniBooNE.

97°

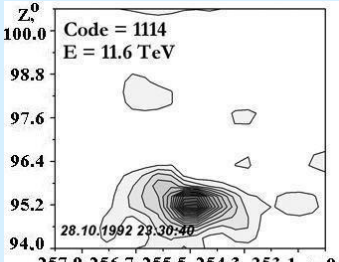

28.10.92
EVENT No 1
23:30:38.27

4	2	7	10	11	13	12	12	0	6	7	0
6	1	0	1	5	5	0	1	5	4	3	4
3	3	1	2	2	4	3	5	1	1	7	3
6	7	0	5	9	2	3	1	5	2	1	7
1	2	4	1	17	14	0	5	5	2	3	3
3	4	4	0	5	5	3	7	11	7	5	6
1	1	0	0	4	5	4	9	1	2	1	1
5	4	0	3	2	16	5	1	11	0	7	16
0	4	6	5	20	47	24	12	5	4	3	3
4	6	2	7	23	43	165	71	17	9	17	2
0	0	3	12	1	25	33	14	20	1	2	1
5	0	6	6	12	13	24	1	0	7	6	5

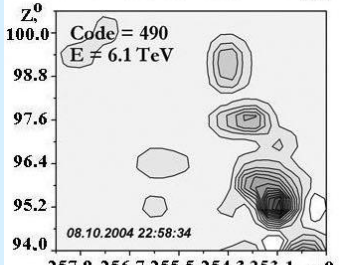

08.10.04
EVENT No 1
22:58:38.27

0	0	0	0	0	0	0	0	0	0	0	0
0	0	5	0	0	0	0	0	0	0	0	0
0	6	0	0	0	0	0	25	0	0	0	0
0	0	0	0	0	0	0	23	0	0	0	0
0	0	0	0	0	0	0	0	0	0	0	0
0	0	0	0	0	0	0	22	38	0	0	0
0	0	0	0	0	0	0	0	0	12	0	0
0	0	0	0	11	5	0	0	14	11	0	0
0	0	0	0	0	0	0	0	50	52	7	0
0	0	0	0	5	0	0	5	8	114	0	0
0	0	0	0	0	0	0	0	0	0	5	0
0	0	0	0	0	0	0	5	7	0	53	0

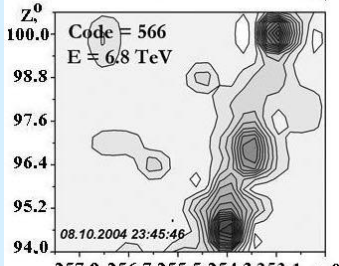

EVENT No 4
23:45:46. 1

0	0	0	0	0	0	0	0	0	0	5	0
0	0	8	0	0	0	0	0	0	67	6	0
0	0	6	0	0	0	0	0	0	18	0	0
0	0	0	0	0	0	0	10	0	8	12	0
0	0	0	0	0	0	0	0	7	10	6	7
0	0	0	0	0	0	0	0	6	17	0	6
0	0	6	6	0	0	0	14	42	5	0	0
0	0	0	0	10	0	0	12	37	6	0	0
0	0	0	0	0	0	0	26	0	0	0	0
0	0	0	0	0	0	0	20	40	17	0	0
0	0	0	0	0	0	0	11	75	0	0	0
0	0	0	8	0	11	11	10	0	0	0	0

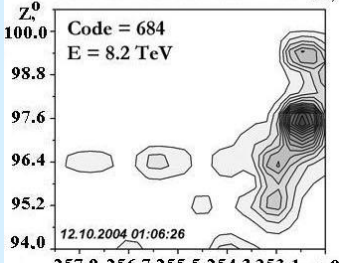

12.10.04
EVENT No 6
1: 6: 7.70

0	0	0	0	0	0	0	0	0	0	0	0
0	0	0	0	0	0	0	0	0	0	0	0
0	0	0	0	0	0	0	0	0	0	48	12
0	0	0	0	0	0	0	0	0	0	13	41
0	0	0	0	0	0	0	0	0	0	21	21
0	0	0	0	0	0	0	0	0	22	134	0
0	0	0	0	0	0	0	0	10	23	74	9
0	5	5	0	15	9	0	11	11	48	18	8
0	0	0	0	0	0	0	0	0	28	7	0
0	0	0	0	0	0	0	5	0	13	32	0
0	0	0	0	0	0	0	0	0	0	5	0
0	0	0	8	0	0	0	21	7	0	0	0

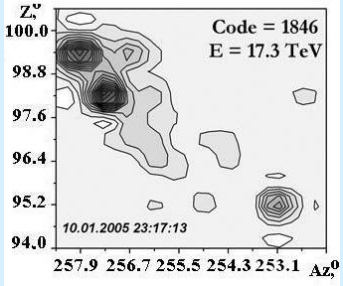

10.01.05
EVENT No 2
23:17: 2. 1

14	17	8	8	0	11	12	11	5	5	0	6
30	0	16	7	0	0	0	0	0	0	0	0
24	246	63	79	23	0	0	0	0	5	0	0
10	68	98	27	11	8	5	0	0	0	0	0
0	7	284	65	45	0	0	13	0	0	18	0
0	10	0	52	23	13	0	0	0	0	0	0
0	9	13	41	43	0	16	19	0	0	0	0
0	0	0	0	41	21	0	19	5	9	13	0
0	0	0	0	0	11	5	0	0	0	0	0
0	0	0	0	16	0	20	5	8	125	8	0
0	0	0	6	0	0	0	0	0	0	0	0
0	0	0	0	6	0	11	12	0	0	0	17

0°

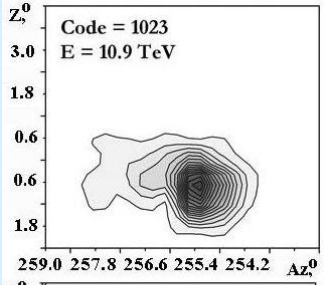

EVENT No 462
2:13:46.33

0	0	0	0	0	0	0	0	0	0	0	0
0	0	0	0	0	0	0	0	0	0	0	0
0	0	0	0	0	0	0	0	0	0	0	0
0	0	0	0	0	0	6	0	0	0	0	0
0	0	0	0	0	0	0	0	0	0	0	0
0	0	0	0	0	0	0	0	0	0	0	0
0	0	9	9	7	12	6	9	0	0	0	0
0	0	6	16	21	37	67	27	8	7	8	0
0	5	12	13	33	44	163	87	20	0	0	0
0	0	11	5	11	12	116	64	13	0	0	0
0	0	0	0	0	8	16	15	0	0	0	0
0	0	0	0	7	8	9	6	0	0	0	0

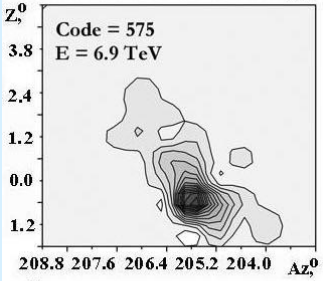

EVENT No 1118
0:37:25.35

0	0	0	0	0	0	0	0	0	0	0	0
6	0	7	9	0	0	0	0	0	0	0	0
0	0	0	0	0	0	0	0	0	0	0	0
0	5	0	0	0	0	0	0	0	0	0	0
0	0	0	0	10	0	0	0	0	0	0	0
0	0	0	0	9	7	0	0	0	0	0	0
0	0	0	5	11	0	9	0	0	0	0	0
0	0	0	0	0	25	22	0	5	0	0	0
0	0	0	0	0	15	52	0	0	0	0	0
0	0	0	0	0	0	115	44	10	0	0	0
0	0	0	0	0	0	0	13	0	0	0	0
0	0	0	0	0	0	0	0	0	0	0	0

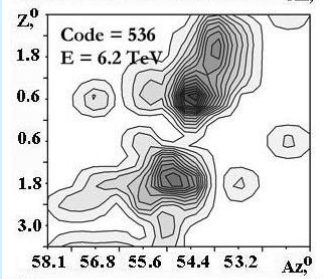

EVENT No 226
2:29:32.92

0	0	0	0	0	0	0	8	0	0	5	0
0	0	0	0	0	0	5	26	11	0	0	0
0	0	0	0	0	0	12	29	11	0	0	0
0	0	0	0	6	8	28	21	9	0	0	0
0	0	8	0	8	11	51	23	0	0	0	0
0	0	0	0	0	0	16	0	0	0	0	0
0	0	0	0	7	0	0	0	0	0	5	0
0	0	0	0	6	28	13	0	0	0	0	0
0	0	7	9	15	34	32	0	5	0	0	0
0	6	5	0	14	6	9	0	0	0	0	0
0	0	0	0	0	9	0	0	0	0	0	0
0	7	7	7	5	5	0	0	0	0	0	0

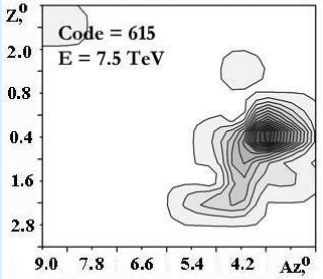

EVENT No 1788
1:23:46. 6

0	0	0	0	0	0	0	0	0	0	0	0
6	5	0	0	0	0	0	0	0	0	0	0
0	0	0	0	0	0	0	0	0	0	0	0
0	0	0	0	0	0	0	0	0	6	0	0
0	0	0	0	0	0	0	0	0	0	0	0
0	0	0	0	0	0	0	0	0	0	43	18
0	0	0	0	0	0	0	0	10	37	103	50
0	0	0	0	0	0	0	0	7	35	20	6
0	0	0	0	0	0	0	0	0	25	8	0
0	0	0	0	0	0	0	11	18	19	0	0
0	0	0	0	0	0	0	0	0	0	0	0
0	0	0	0	0	0	0	0	0	0	0	0

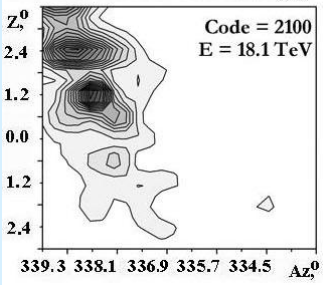

EVENT No 328
23: 8:49. 5

162	198	67	7	0	0	0	0	0	0	0	0
34	101	40	12	0	0	0	0	0	0	0	0
47	247	206	93	17	0	0	0	0	0	0	0
13	44	63	24	33	15	0	0	0	5	6	0
25	65	294	60	28	0	6	0	0	0	0	0
9	67	70	119	15	0	0	0	0	0	0	0
7	21	22	28	32	0	8	0	0	0	0	0
7	14	37	60	0	9	5	0	0	0	0	0
0	0	20	23	34	20	10	0	0	0	0	0
5	6	25	12	20	0	5	0	0	20	0	0
0	0	10	8	15	19	7	5	0	0	0	0
0	0	0	0	6	0	0	0	5	0	0	0

Conclusion

- We presented the results of observations of two types of **Galactic** supernova remnants with the SHALON mirror Cherenkov telescope of Tien-Shan high-mountain Observatory: the shell-type supernova remnants Cas A, Tycho, γCygni SNR, and IC 443; plerions Crab Nebula, 3c58(SN1181) and Geminga (probably plerion). The experimental data have confirmed the prediction of the theory about the hadronic generation mechanism of very high energy γ-rays in Tycho's supernova remnant. The data obtained suggest that the TeV γ-ray emission in the objects being discussed is different in origin.
- During the period 1992 - 2014, SHALON has been used for observations of the **metagalactic** sources NGC1275 (z=0.0179), Mkn421 (z=0.031), Mkn501 (z=0.034), Mkn180 (z=0.046), 3c382 (z=0.0578), 4c+31.63 (z=0.295), OJ 287 (z=0.306), 3c454.3 (z=0.859), 4c+55.17 (z=0.896), 1739+522 (z=1.375).
- We presented the results of fifteen-year-long observations of the AGN NGC 1275 at energies 800 GeV–40 TeV discovered by the SHALON telescope in 1996. The data obtained at very high energies, namely the images of the galaxy and its surroundings, and the flux variability indicate that the TeV γ-ray emission is generated by a number of processes: in particular, part of this emission is generated by relativistic jets in the nucleus of NGC 1275 itself. Whereas, the presence of an extended structure around NGC 1275 is evidence of the interaction of cosmic rays and magnetic fields generated in the jets at the galactic center with the gas of the Perseus cluster.
- The detection of TeV γ-ray sources at high red-shifts is the evidence of less average spectral density of **Extragalactic Background Light** and thus the less star formation rate at early evolution stage, than it is previously believed. Also, the possible explanation of the detected very high energy γ-emission from the distant AGNi is the re-scattering of primary TeV-photons on the Dark Matter particles, so called WISP – weakly interacting slim particles. The axion-like particles has been considered to be a candidate for such weakly interacting slim particles.
- **During 350 hours of observations at 97º zenith angle** after a cut of shower-like events that may be caused by chaotic sky flashes or reflections on the snow of vertical showers, we have detected 5 air showers of TeV energies. These events may be caused by the decay of a long-lived penetrating particle entering the atmosphere from the ground and decaying in front of the telescope. As a possible explanation, scenarios with an unstable neutrino of mass $m \approx 0.5$GeV and $c\tau \approx 30$ m are discussed. One of these models has been recently proposed to explain an excess of electron-like neutrino events at MiniBooNE.